aer

NASA CR- 177833

ATMOSPHERIC AND ENVIRONMENTAL RESEARCH, INC.
CAMBRIDGE, MASSACHUSETTS

ADVANCED MOISTURE AND TEMPERATURE

SOUNDER (AMTS) STUDY

Final Report

NASA Contract NAS5-27629

Prepared by

L. D. Kaplan, R. G. Isaacs, R. D. Worsham, and G. DeBlonde

Atmospheric and Environmental Research, Inc.
840 Memorial Drive
Cambridge, Massachusetts 02139

Prepared for

Laboratory for Atmospheric Sciences
NASA Goddard Space Flight Center
Greenbelt, MD 20771

June 1985

TABLE OF CONTENTS

LIST OF TABLES

LIST OF FIGURES

ABSTRACT

Retrieval of tropospheric humidity profiles from satellite-based upwelling radiances are shown to be improved by using physical methods for obtaining first-guess profiles as well as for inverting the radiative transfer equation by relaxation. The first guess is based on an empirically verified hypothesis, from theoretical considerations, that the brightness temperature corresponding to the radiance should be approximately equal to the actual temperature at a channel-invariant optical depth provided that the surface and stratospheric contributions to the radiance are small.

Even greater improvement of retrieved humidity profiles can be accomplished by increasing the number of channels used and by selecting their spectral location and bandpass to obtain sharper independent weighting functions. For example, the AMTS system, with high resolution water channels at 1650, 1700, 1839, 1850 and 1930 cm^{-1}, is shown to be capable of reducing the retrieved water vapor errors in 200 mb thick layers by a factor of two to three relative to the HIRS-2 system errors. Expected AMTS errors in tropical layer water content are particularly low, less than 20% at all levels, and of the order of 10% or less in the middle troposphere.

Statistical retrievals were carried out and were generally better than the physical retrievals in the lower and upper troposphere but were worse in the middle troposphere. When all channels were used, AMTS gave slightly better results than HIRS at all heights. The AMTS was distinctly better when only the moisture channels were used. The results of these studies indicate that the AMTS system is superior, but that it can be further improved by meshing physical and statistical retrievals and by using more moisture-sensitive channels in the 15 μm CO_2 band.

A test of the usefulness of new channels extending the height to which atmospheric water vapor can be routinely retrieved will require confirming measurements beyond the present radiosonde limits. ATMOS data should be useful for this purpose.

1. INTRODUCTION

The aim of this effort was to optimize the selection of channels for the Advanced Moisture and Temperature Sounder (AMTS). The initial emphasis was to be on the water vapor channels, but the study was to include investigation of the possibility of finding two ozone channels giving independent stratospheric and tropospheric ozone distribution, and the dependence of temperature retrievals on spectral resolution.

Work on the contract tasks had already begun before the effective starting date with support from Jet Propulsion Laboratory. In particular, we had found two superior water vapor channels, at 1650.1 and 1700.3 cm^{-1}, to replace the old upper troposphere channels at 1844.5 and 1889.57 cm^{-1}. This substitution gives sharp weighting functions evenly spaced throughout the troposphere. A window channel at 875.0 cm^{-1} was found to be a better choice than the one at 1203.0 cm^{-1} which was redundant with the 1232 cm^{-1} channel. The search for a second, nonredundant ozone channel was unsuccessful, but the location of the one channel was optimized to 1040.8 cm^{-1}. The new channel locations appeared in several reports (e.g., Chahine et al., 1984) and are reproduced in Table 1.

Midway in the originally planned research period, NASA decided to terminate AMTS studies. Because of this, almost all of the effort was devoted to the water vapor channels, and even that investigation is incomplete with interesting possibilities still to be pursued.

Section 2 of this report describes the data, algorithms, and methodology used in the study, presents water vapor weighting functions and the results of sensitivity studies, and shows the relationships between channel brightness temperatures and transmittance or integrated water. These lead to a new first-guess algorithm, which is introduced and investigated in Section 3. Section 4 reports on simulated retrievals by relaxation, and shows that the AMTS moisture channels are potentially capable of providing substantially better retrievals than the HIRS channels. Figure 1-1 is a schematic of the moisture retrieval process including first guess and relaxation codes. Section 5 shows the results of retrieval simulations with statistical regression, which again indicates advantages of the AMTS relative to HIRS and, at least for clear-column radiances, relative to AMSU for tropospheric water vapor retrievals. Section 6 includes a summary discussion and suggestions for future investigations.
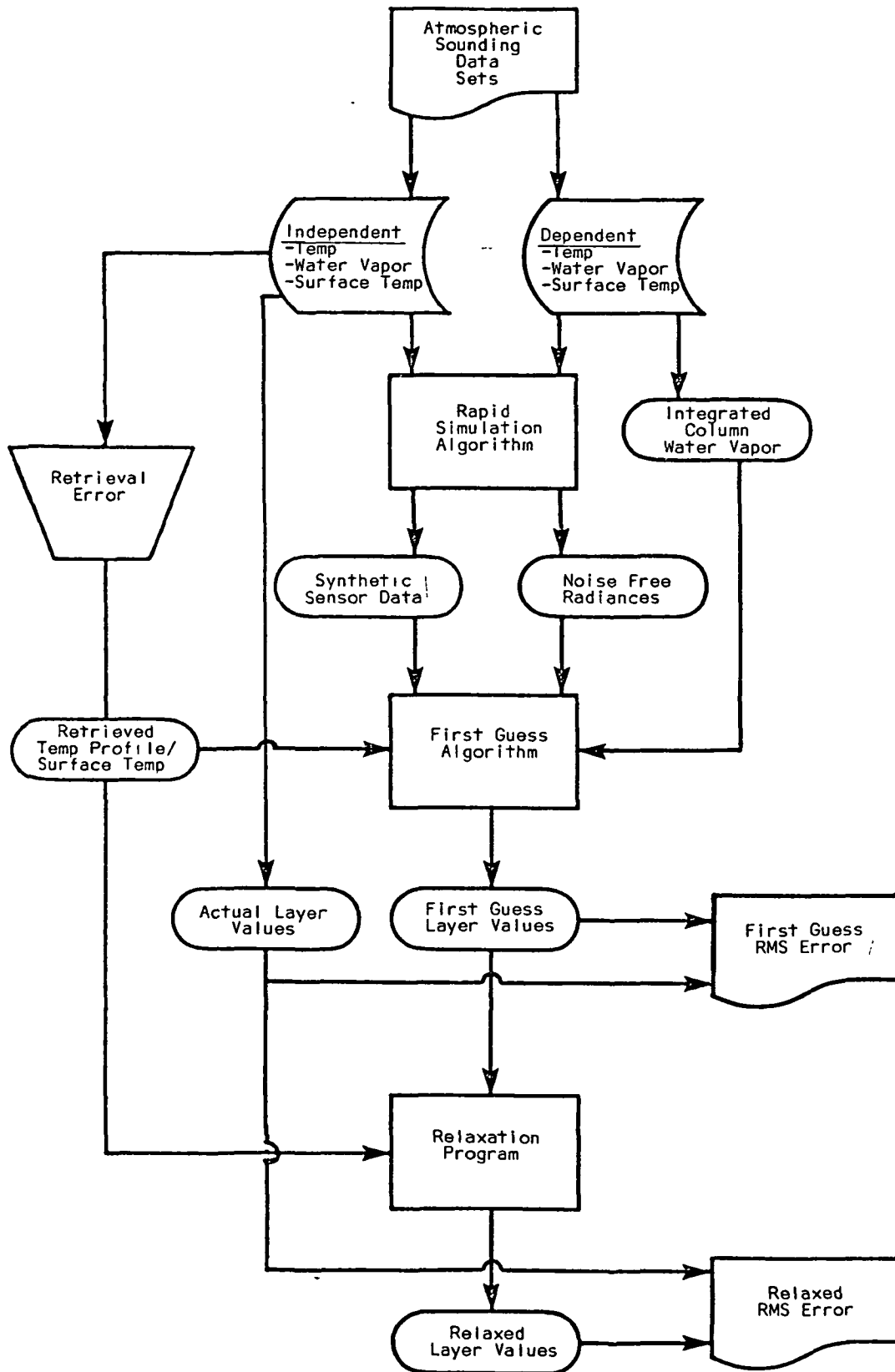
Figure 1-1.   Schematic of Moisture Retrieval Process Including First
Guess and Relaxation Codes

TABLE 1 AMTS NARROW BAND PASS CHANNELS

Band	Channel	Channel Wavelength	Spectral Frequency	Half-power Spectral Resolution	Equivalent Scene Blackbody Temperature Above Atmosphere			Main Channel Function
No.	No.	λ(μm)	υ(cm^{-1})	$\Delta\upsilon$(cm^{-1})	T_{min}	T_{std}	T_{max}	
1	1	16.476	606.95	0.50	230	263.83	286	CLOUD FILTERING
	2	16.046	623.20	0.50	229	260.15	283	
	3	15.929	627.80	0.50	218	236.51	260	
	4	15.765	634.30	0.50	211	226.46	256	
	5	15.466	646.60	0.50	202	219.66	248	
	6	15.282	654.35	0.50	195	219.68	255	TEMPERATURE PROFILE UPPER ATMOSPHERE
	7	15.025	665.55	0.50	197	222.69	266	
	8	14.996	666.85	0.50	194	223.38	279	
	9	14.967	668.15	0.50	198	254.00	300	
	10	14.938	669.45	0.50	199	233.04	285	
2	11	11.429	875.00	0.75	231	285.00	327	H_2O/SST
	12	9.608	1040.80	1.00	198	256.26	290	OZONE
	13	8.120	1231.60	1.00	231	285.40	327	H_2O/SST
	14	6.060	1650.10	1.30	220	--	261	H_2O PROFILE
	15	5.881	1700.30	1.30	216	--	255	
3	16	5.437	1839.40	1.50	232	259.32	282	H_2O PROFILE
	17	5.403	1850.90	1.50	233	266.90	289	
	18	5.181	1930.10	1.50	232	280.28	315	
4	19	4.195	2384.00	2.00	214	229.56	274	TEMPERATURE PROFILE LOWER ATMOSPHERE
	20	4.191	2386.10	2.00	222	240.97	299	
	21	4.187	2388.20	2.00	229	254.69	313	
	22	4.184	2390.20	2.00	231	265.88	321	
	23	4.180	2392.35	2.00	232	273.30	325	
	24	4.176	2394.50	2.00	232	276.20	326	
	25	4.125	2424.00	2.50	232	281.38	331	AIR-SURFACE ΔT
	26	3.992	2505.00	2.50	232	285.22	342	SKIN SURFACE TEMPERATURE
	27	3.822	2616.50	2.50	232	286.57	354	
	28	3.723	2686.00	2.50	232	286.53	364	

2. AMTS SIMULATIONS

2.1 Simulation Methodology and Algorithms

As a prerequisite to our channel optimization studies, a variety of computational tools were implemented on AER's in-house Harris computer. These codes provided the capabilities to: (1) generate and maintain files of spectral data for desired atmospheric absorbers and wavenumber intervals, (2) accurately evaluate channel atmospheric transmission, weighting functions, and emergent radiances and brightness temperatures using the line-by-line (LBL) approach and spectral data obtained in (1) above, and (3) perform efficient sensor radiance/brightness temperature simulations using a "rapid" atmospheric transmittance algorithm based on the LBL results. Since none of the codes referred to above were written on Harris compatible machines each required program conversion, testing, and where possible, comparison with test cases.

The models described above were exercised to perform a variety of calculations during the current reporting period including: (1) water vapor channel brightness temperature simulations, (2) evaluation of channel weighting functions, and (3) sensitivity analyses. The theme of these studies has been the investigation of the response of selected water vapor channels to changes in temperature and moisture profile.

2.1.1   Spectral Data

Our spectral data base is the most recent version of the AFGL compilation of absorption line (molecules 1-7) and trace gas (molecules 8-28) parameters obtained from AFGL (Rothman et al., 1983). Two separate programs were used to access this data and generate input files for calculations with Susskind's (1978) LBL code and the AFGL FASCODE (Smith et al., 1978), respectively. In the former case, formatted spectral data "BFILES" have been generated for use in the following wavenumber regions: 0-100, 500-900, 600-1400, 1250-2400, 2100-2900 cm^{-1}. (The first of these was used in a modified version of the LBL code which we have used to perform microwave simulations.) Binary spectral data sets for FASCODE were prepared using our converted version of AFGL's "BCDMRG" program which provides the added capability to select trace gases of interest and merge them by wavenumber into the desired data set.

2.1.2   Line-by-line Codes

We used our converted version of Susskind's LBL code for exact calcu-
lations of channel transmittance and weighting function profiles and to
simulate sensor-incident radiances. This code originally came to us in CDC
compatible FORTRAN format, accompanied by an update file providing for radi-
ance calculations, a Gaussian filter function, and the nitrogen and water
vapor continua. Since our system does not include update file capabilities,
these changes were hand edited into the source code using a complete listing
for guidance and previous model runs for verification. Modified versions of
this code were written to: (1) perform sensor channel sensitivity analyses
(described in 2.3 below), (2) calculate transmittance and weighting functions
over narrow (0.1 cm^{-1}) band passes to aid in the search for optimum channel
locations, and (3) extend the infrared code to the 0-100 cm^{-1} spectral region
for microwave simulations. This last task largely involved changes in
spectral data format, substitution of the van Vleck-Weisskopf line shape, and
specification of the microwave water vapor continuum expression used by Gaut
and Reifenstein (1971).

Additionally, we obtained and converted the high resolution fast atmo-
spheric signature code (FASCODE) developed at AFGL (Smith et al., 1978) for
eventual use in our simulations. The version is denoted FASCOD1C (Clough,
1983). Test cases provided have been successfully verified and comparisons
with the Susskind (i.e., project) LBL code described above carried out.

2.1.3   Rapid Algorithm

The rapid algorithm for modeling atmospheric transmittance and radiance
described by Susskind et al. (1982) has been obtained in addition to required
input data sets including winter and summer extrapolated radiosonde profiles
(i.e., the Phillips data) and transmittance functions for the HIRS/MSU and
AMTS/MSU. This code has been converted to run on the Harris computer and
results compare favorably to sample output of brightness temperatures
generated by the simulation program which were provided by NASA.
(Discrepancies are on the order of the Gaussian noise added in the
simulation.) Additionally, favorable comparisons were made to previous
calculations using the LBL code. Modifications have been made to the rapid
simulation code to: (1) evaluate weighting function profiles using a method
analogous to that in the project LBL code, (2) perform sensitivity analyses to

layer water vapor and temperature variations (described below),
(3) accommodate the recently supplied transmittance function coefficients for
the new AMTS channels (i.e., 875, 1650.1, 1700.3 cm^{-1} at nadir including
appropriate changes to the water vapor continuum self broadening
coefficients), and (4) accept climatological model profiles (from the "WPOT"
data set) in addition to the radiosonde profiles (read by subroutine
"FIDRAD").

2.2 AMTS Channel Weighting Functions

Weighting functions were evaluated for a subset of the thirty-two
seasonally (1=winter, 2=spring, 3=summer, 4=fall) and latitudinally (1=0°,
2=10°, 3=20°, ..., 8=70°) dependent atmospheres from Rodgers (1967) supplied
as the "WPOT" climatological data set. Figure 2-1 illustrates these results
for the AMTS water vapor channels as a function of season at the equator.
Results for the seasonal variation of the channel at 1839.4 cm^{-1} at latitude
40° are illustrated in Figure 2-2. Among other features, a shift of peak
sensitivity pressure level with seasonal water vapor variation is evident.
The variation of AMTS water vapor weighting functions with latitude is
illustrated in Figure 2-3. These calculations were done for a spring
atmosphere at the equator, 20°N, 40°N, and 60°N. The change in shape of
individual channel weighting functions and shifting of weighting function peak
pressure levels to higher pressures at higher latitudes is notable. In a
practical context, these results emphasize that individual channels are
sensitive to water vapor at pressure levels which differ systematically in the
course of a satellite orbit. As has been suggested by other investigators,
for this reason it is useful to consider water vapor weighting functions in an
alternative coordinate system based on integrated absorber amount (Chahine,
1970; Rosenkranz et al., 1982; Rosenberg et al., 1983). This is further
illustrated in Figure 2-4 which plots channel weighting functions, WF_i,
defined as:

$$WF_i = \frac{d\tau^i}{d\ln U_i} \tag{2.1}$$

vs. column integrated water vapor, V_i, for three model January atmospheres for
latitudes: (a) 0°, (b) 40°N, and (c) 60°N. In this representation weighting
functions remain approximately constant among model atmospheres.
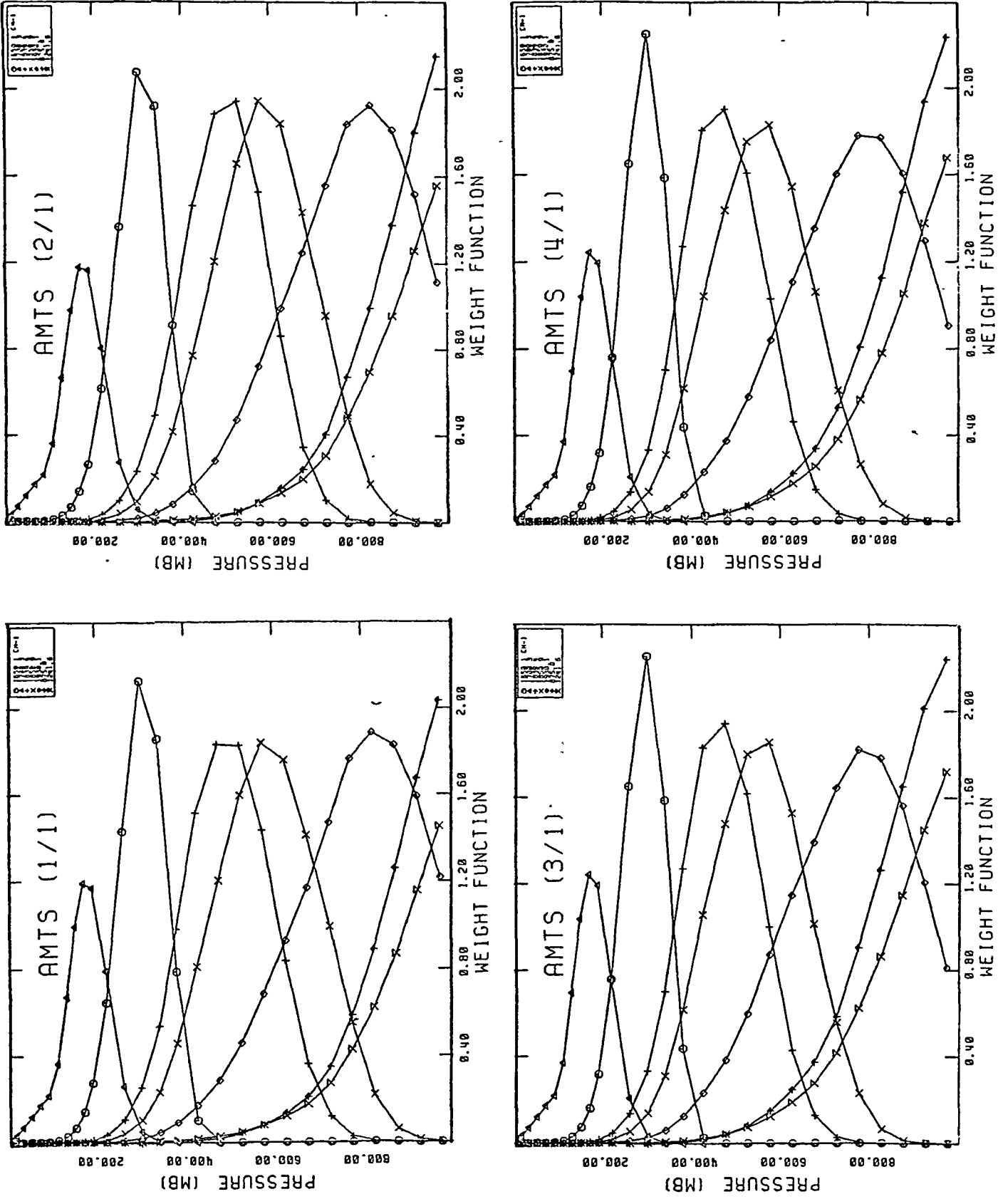
Figure 2-1. AMTS water vapor channel weighting functions at equator for winter (1/1), spring (2/1), summer (3/1), and fall (4/1).
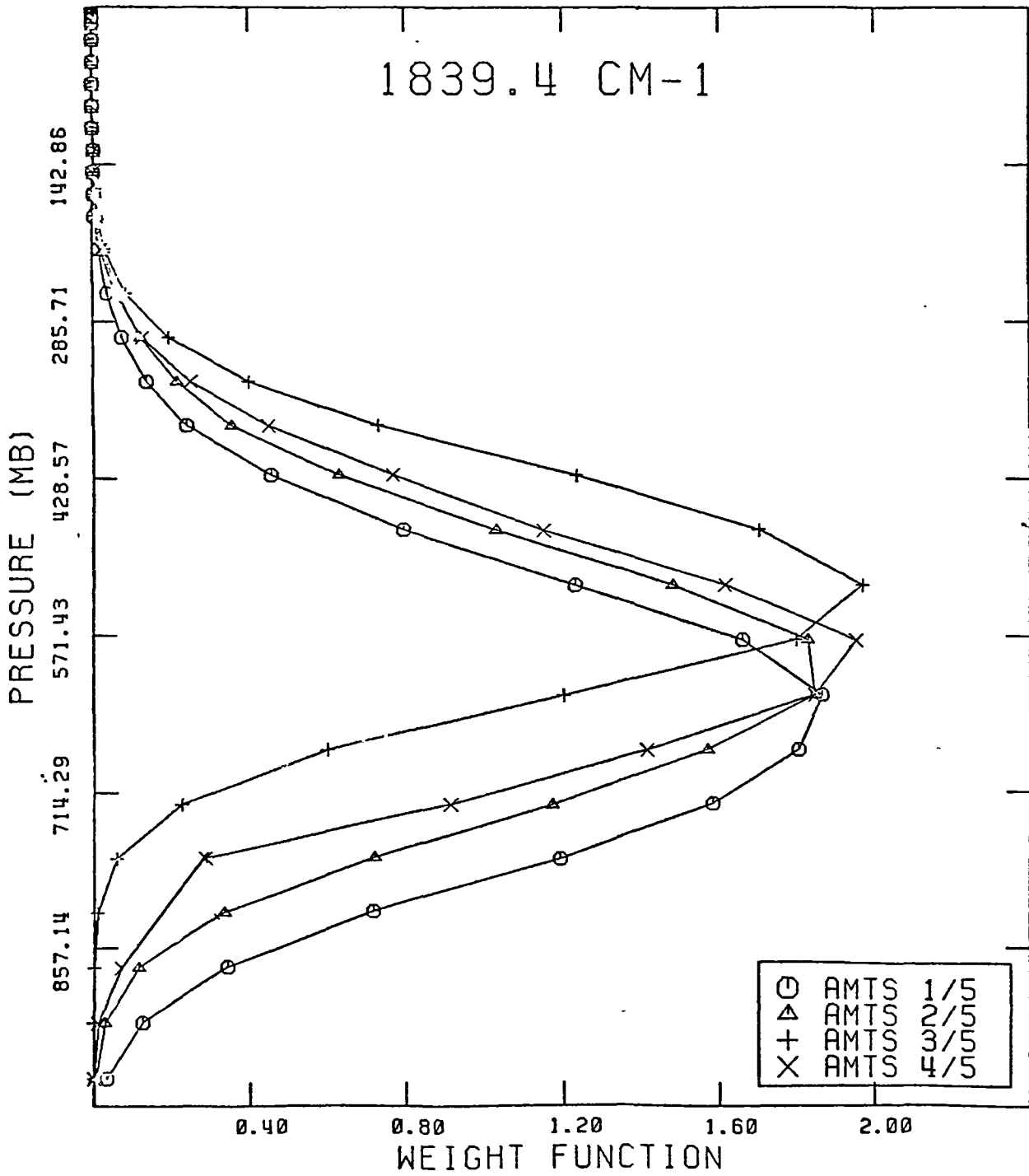
Figure 2-2. Dependence of 1839.4 cm^{-1} channel on season at 40°N
latitude: winter (1/5), spring (2/5), summer (3/5),
and fall (4/5).
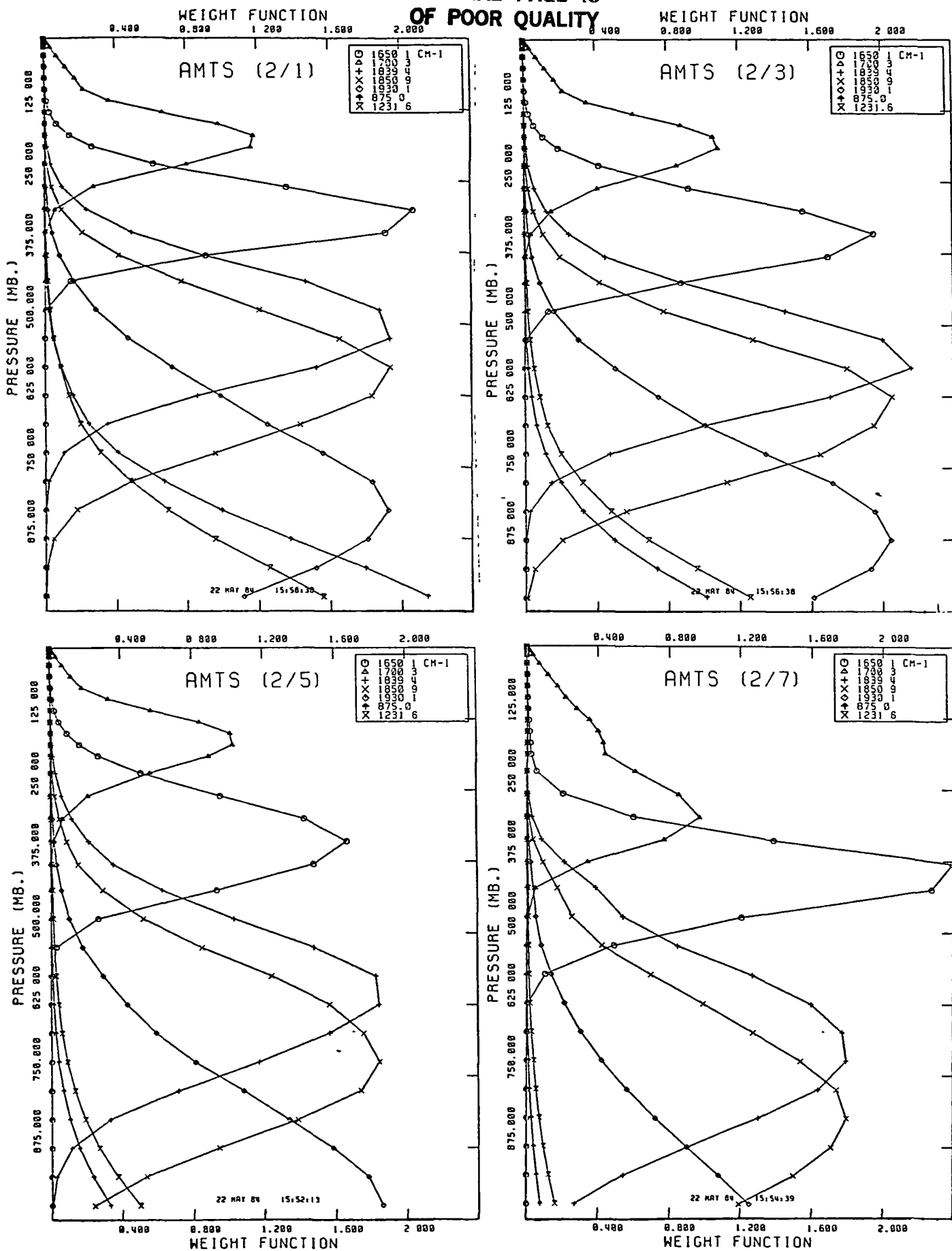
Figure 2-3. Spring AMTS water vapor channel weighting functions for the equator
(2/1), 20°N (2/3), 40°N (2/5), and 60°N (2/7).
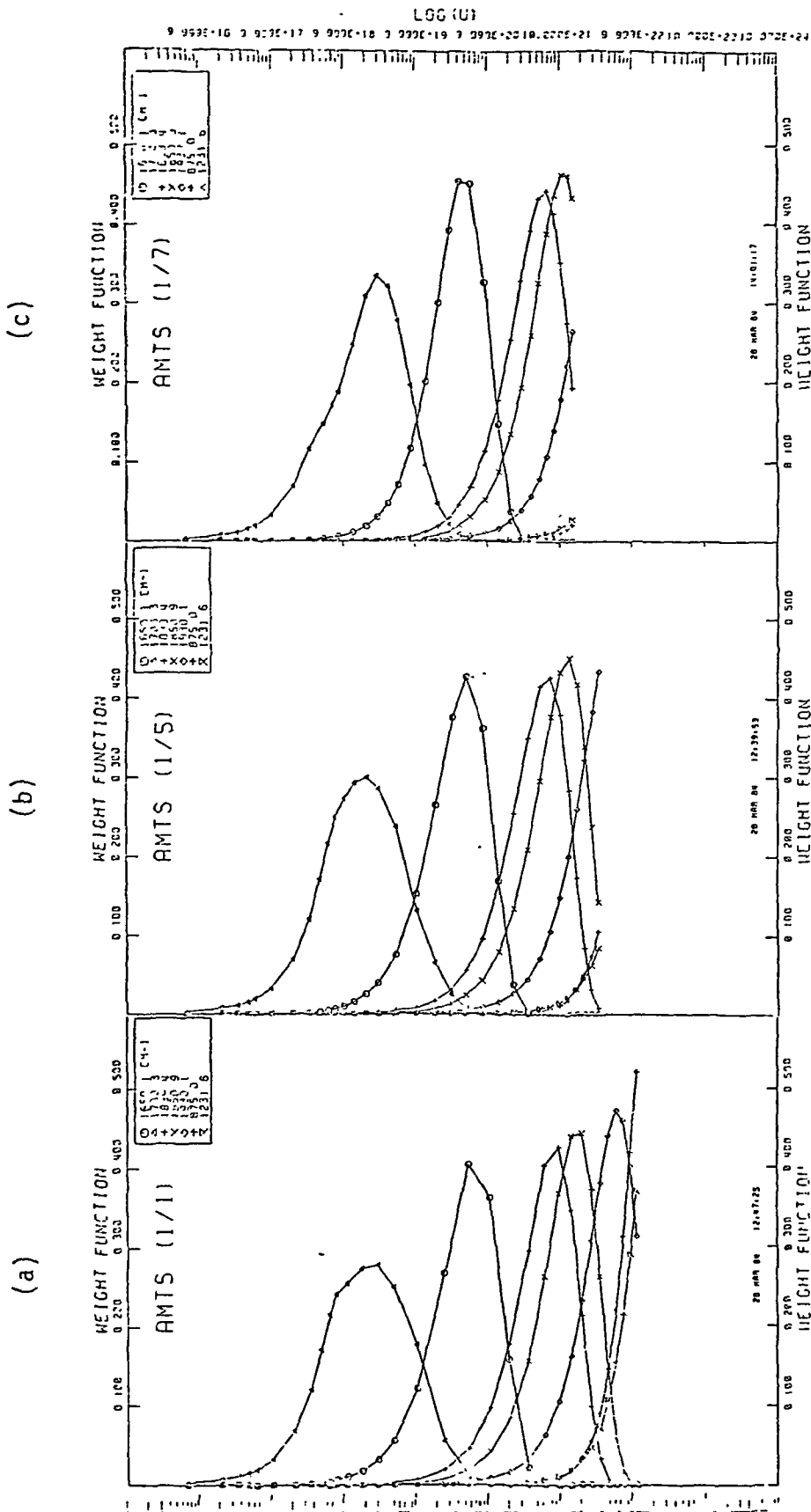
Figure 2-4. AMTS channel weighting functions vs. column integrated water vapor for three model winter atmospheres at the equator (1/1), 40°N (1/5), and 60°N (1/7).

2.3 Sensitivity Studies

The computational efficiency of the rapid simulation algorithm provided an opportunity to perform a variety of sensitivity studies which would not ordinarily be undertaken using a time consuming LBL approach. An example is the set of sensitivity calculations described below.

The purpose of these calculations was to examine the sensitivity of the AMTS water vapor channels to specified changes in temperature and water vapor abundance at individual layers within the atmosphere. The results of this exercise provide a direct indication of the sensor-incident signal available due to specified changes in the layer values of atmospheric temperature and moisture. Water vapor abundance and temperature were increased by triangular functions with maxima of 20% and 2K, respectively, and 50 mb half-width at half-height, centered within seven 200 mb layers located at 200, 350, 500, 650, 800, 900, and 1000 mb. The algorithm employed was to: (1) select a baseline (i.e. unperturbed) model atmospheres from the "WPOT" data set [designated as (i/j) where i=1,4 is the season and j=1,8 is the latitude, as above], (2) simulate corresponding brightness temperatures for each water vapor channel (i.e., 875, 1231.6, 1650.1, 1700.3, 1839.4, 1850.9, 1930.1 cm^{-1}), (3) increment temperature within the first layer (i.e., centered at 200 mb) and reevaluate channel brightness temperatures, and (4) subtract the set of brightness temperatures obtained in step (3) from that of step (2) for the brightness temperature change due to the perturbation at this pressure level. Steps (3) and (4) are then successively repeated for each layer (i.e., six more times). The process is then repeated for layer water vapor perturbations, resulting in a total of fifteen simulations of the channel set. These calculations with the rapid algorithm compared quite favorably with those reported earlier for a standard atmosphere performed using the LBL code. Due to the time savings it was possible to accomplish the analysis for sixteen model atmospheres (four seasons and latitudes of 0, 20, 40, and 60°). For example, temperature and water vapor sensitivity results for summer, equatorial and spring, midlatitude atmospheric models are shown in Figures 2-5 and 2-6, respectively. There is notable variation of channel sensitivity to both season and latitude. These variations are most apparent comparing the entire set of results for temperature and water vapor. These are illustrated in Figures 2-7a and b, respectively.

TEMPERATURE SENSITIVITY (3/1)

WATER VAPOR SENSITIVITY (3/1)
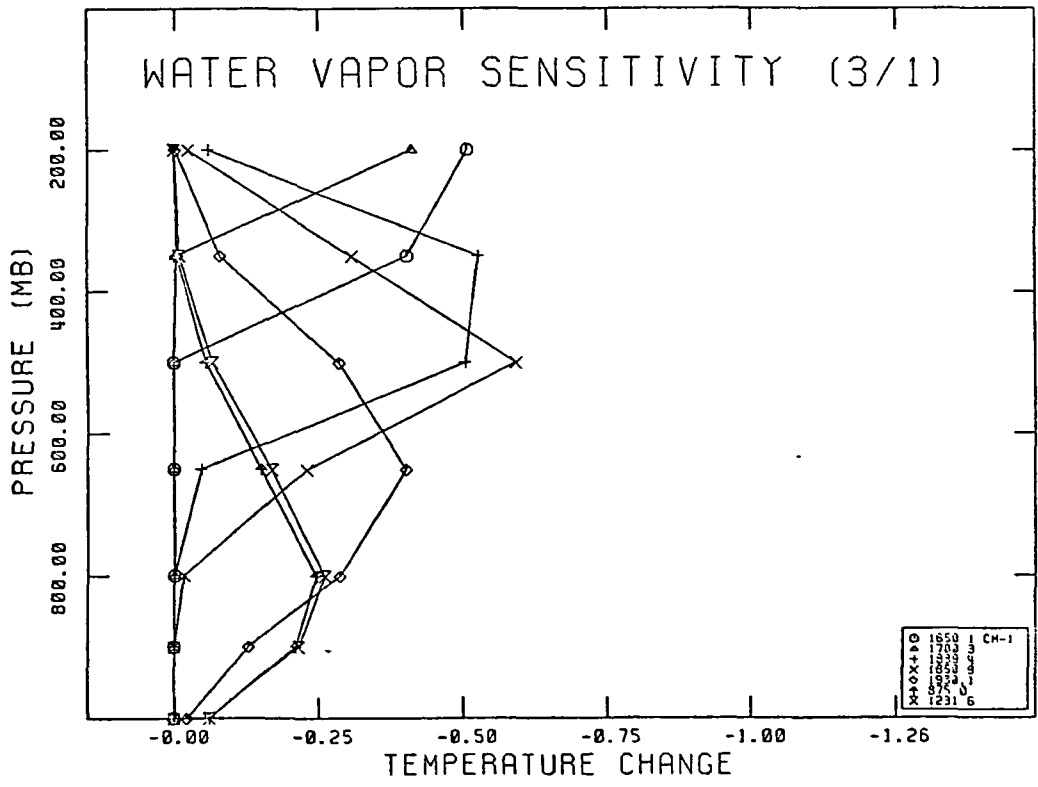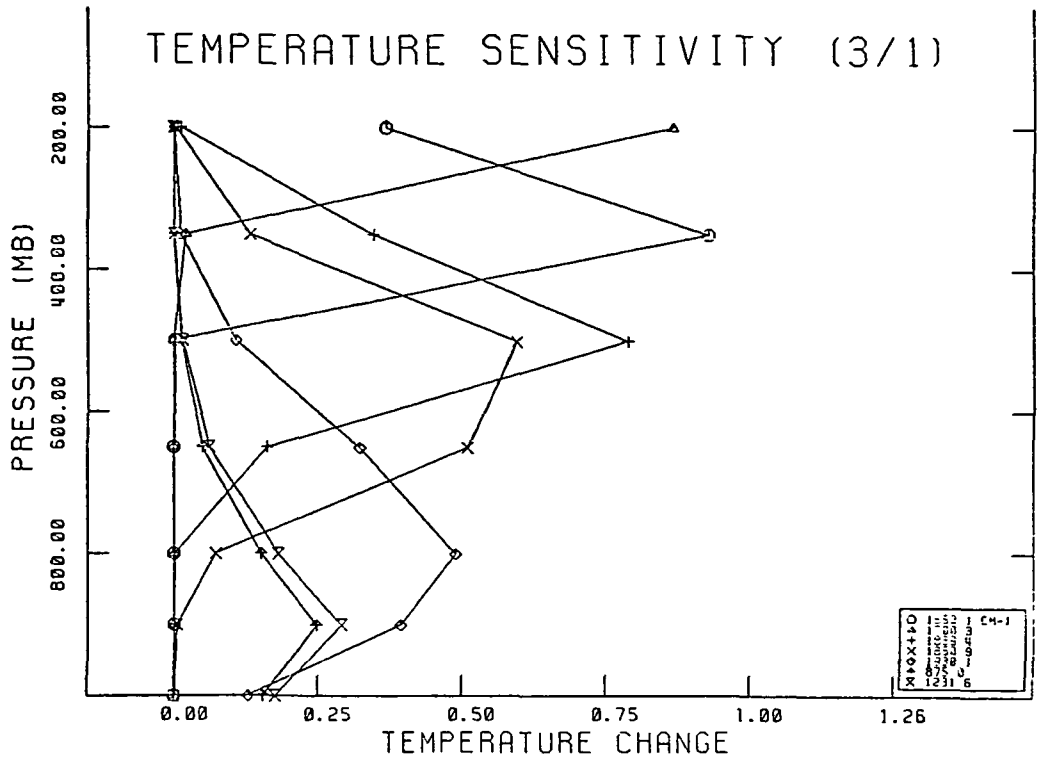
Figure 2-5. Sensitivity of AMTS channels to local changes in layer
temperature and water vapor for a summer equatorial
atmospheric model.

-13-
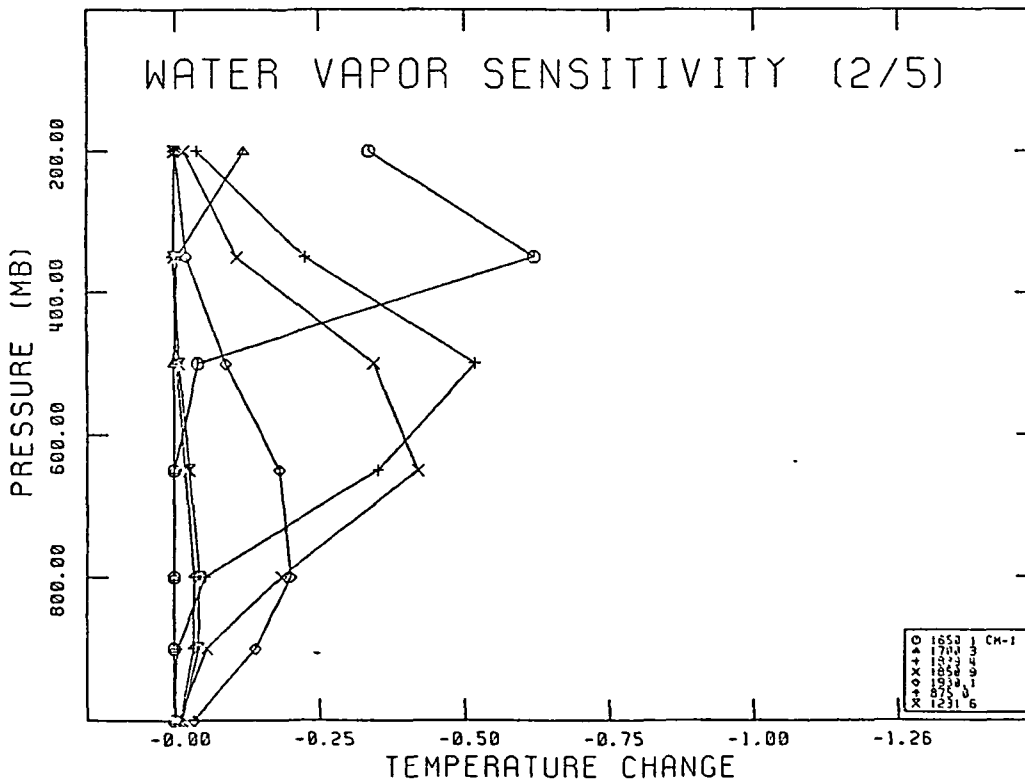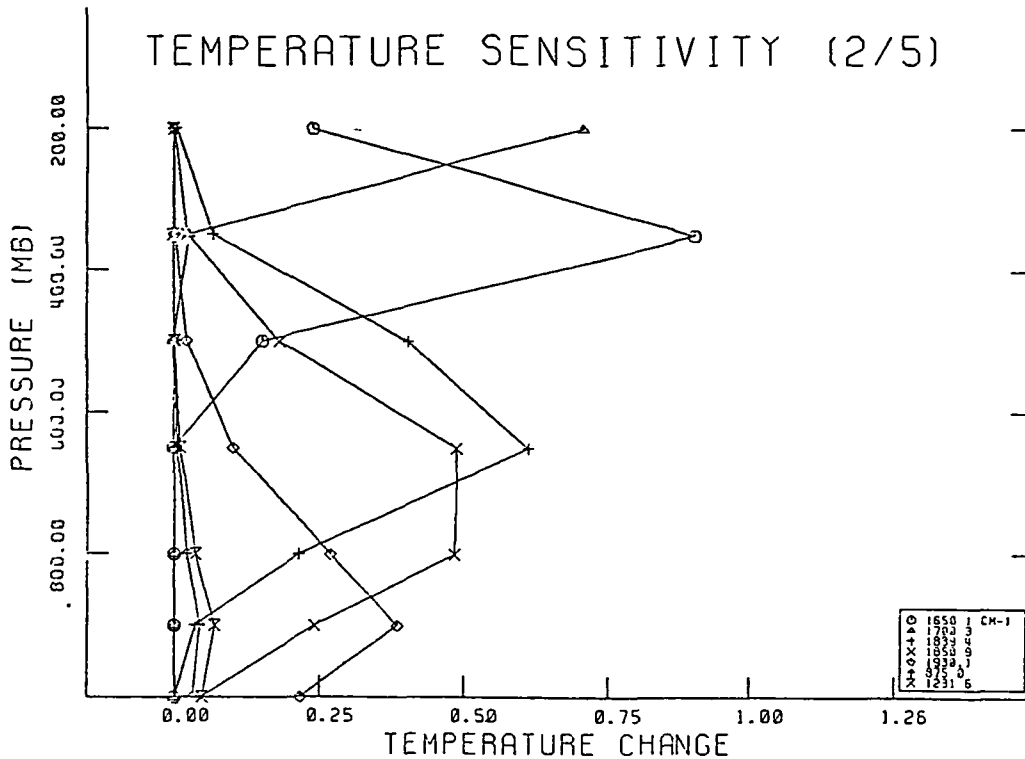
Figure 2-6. Sensitivity of AMTS channels to local changes in
layer temperature and water vapor for a spring
midlatitude (40°N) atmospheric model.

-14-
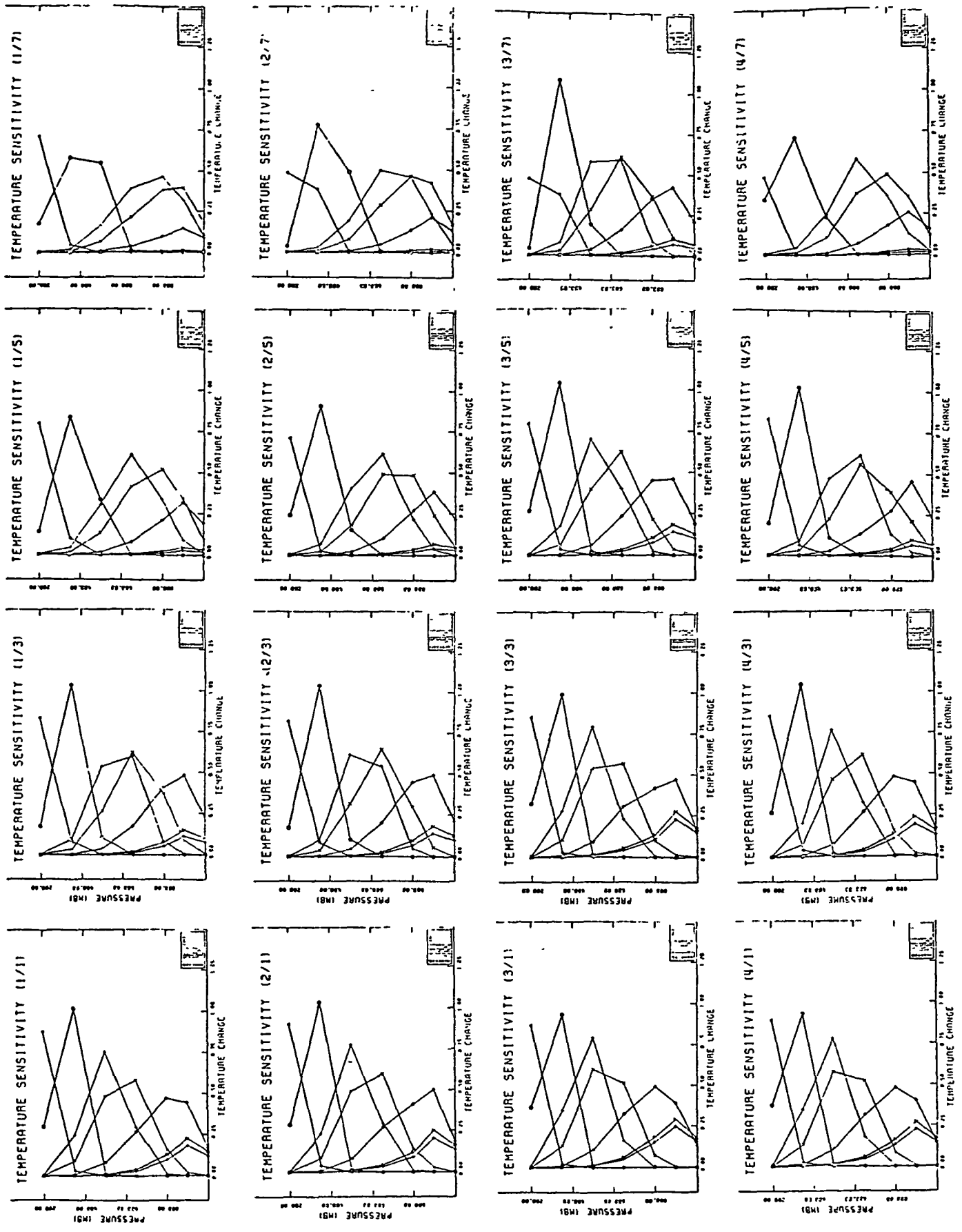
Figure 2-7a. Dependence of AMTS channel sensitivity to layer changes in temperature on season and latitude.

-15-
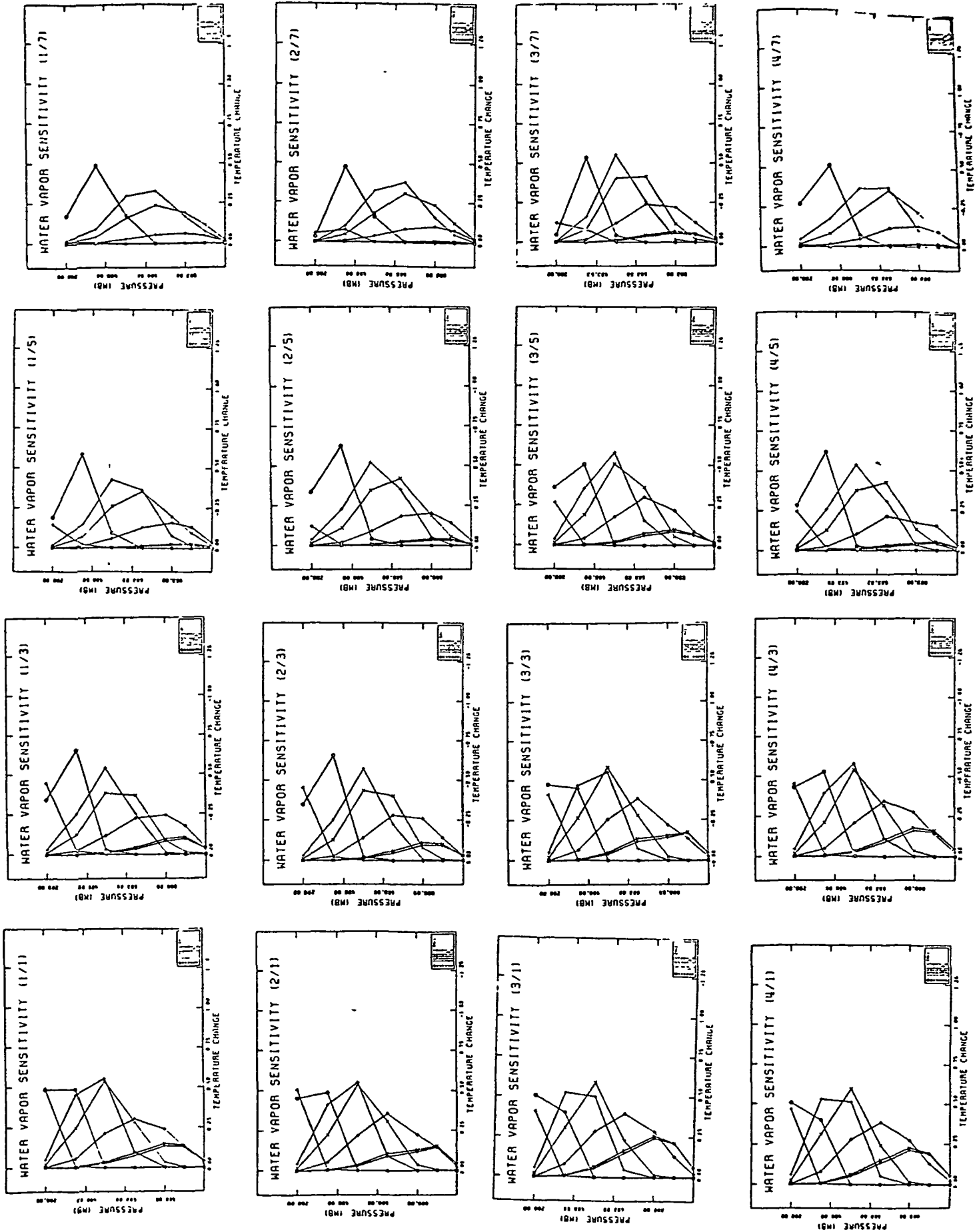
Figure 2-7b. Dependence of AMTS channel sensitivity to layer changes in water vapor on season and latitude.

2.4 Brightness Temperature Simulations

2.4.1 Atmospheric Sounding Sample Sets

Simulated AMTS water vapor channel brightness temperatures are desired both to investigate the relationship between emergent radiances and various properties of the atmospheric water vapor profile and to provide synthetic satellite sensor data for use in subsequent retrieval studies. For these purposes it was desired to work with actual atmospheric soundings rather than climatological data sets such as those described in Section 2.2. The sample of sounding data chosen for this purpose was the Phillips (1984) winter/summer radiosonde set used in the AMTS/HIRS comparison study. The extrapolated profiles supplied by NASA were used instead of the actual incomplete soundings. From among the available 1600 soundings, four sets of 200 atmospheres each were selected corresponding to tropical winter (TW) and summer (TS) and midlatitude winter (MW) and summer (MS), respectively. Within each set the first 100 soundings were designated as the dependent (D) subset to be used as climatology, while the second 100 soundings were designated the independent (I) subset. Brightness temperatures generated from the dependent subset were calculated without adding instrumental noise to provide a basis for relating brightness temperature variations to changes in the vertical distribution of atmospheric water vapor. Noisy brightness temperatures generated from the independent set were subsequently used as synthetic satellite sensor data to test our retrieval methods. Additionally, the tropical winter (TW) set was specially processed to provide a fifth set including soundings over ocean only. In order to accomplish this, the first two-hundred tropical winter soundings over the ocean were identified and alternately sorted into dependent and independent sets. The attributes of the various sample sets described above including sounding header number, approximate latitude range, and land/ocean flag are summarized in Table 2-1.

For each individual sounding, values of temperature (K), water vapor and ozone local column densities (cm^{-2}) are given at 64 pressure levels. The surface temperature is taken as that at the 1000 mb level. Table 2-2 illustrates a sample sounding taken from the TW set. Included is the column integral of water vapor from the top of the atmosphere to a particular pressure level (cm^{-2}). For each individual sounding, column water vapor densities were calculated for five layers corresponding to pressure level

Table 2-1

Attributes of Atmospheric Sounding Sets
Used in Water Vapor Retrievals

Atmosphere Sample*	Sounding Numbers	Latitude Range	Land (L)/ Ocean (O)
Tropical Winter (TW)			
D	1001-1100	-28/-12	L/O
I	1101-1200	-28/+8	L/O
Midlatitude Winter (TW)			
D	1451-1550	+32/+48	L/O
I	1551-1650	+42/+48	L/O
Tropical Summer (TS)			
D	2001-2100	-30/-12	L/O
I	2101-2200	-28/+8	L/O
Midlatitude Summer (MS)			
D	2451-2550	+32/+48	L/O
I	2551-2650	+42/+48	L/O
Tropical Winter (Ocean only)			
D	1001-1317	-28/+28	O
I	1002-1318	-28/+28	O

*Dependent set (D) — first-guess formulation
 Independent (I)   — retrieval application

Table 2-2

Typical Sounding and Water Vapor Column Integral

PRESSURE	TEMPERATURE	WATER	INTEGRAL
1.00	274.727	0.681700E+17	0.681700E+17
2.00	257.724	0.681700E+17	0.136340E+18
3.00	246.825	0.681700E+17	0.204510E+18
4.00	240.710	0.681700E+17	0.272680E+18
5.00	236.087	0.681700E+17	0.340850E+18
6.00	233.349	0.681700E+17	0.409020E+18
7.00	231.233	0.681700E+17	0.477190E+18
8.00	228.563	0.681700E+17	0.545360E+18
9.00	226.210	0.681700E+17	0.613530E+18
10.00	224.677	0.681700E+17	0.681700E+18
15.00	219.095	0.340850E+18	0.102255E+19
20.00	214.789	0.340850E+18	0.136340E+19
30.00	210.520	0.681700E+18	0.204510E+19
40.00	204.069	0.681700E+18	0.272680E+19
50.00	199.089	0.681700E+18	0.340850E+19
60.00	195.132	0.681700E+18	0.409020E+19
70.00	196.043	0.681700E+18	0.477190E+19
80.00	196.587	0.681700E+18	0.545360E+19
90.00	196.891	0.681700E+18	0.613530E+19
100.00	195.024	0.681700E+18	0.681700E+19
110.00	195.429	0.100962E+19	0.782662E+19
120.00	199.316	0.144276E+19	0.926938E+19
130.00	202.892	0.200122E+19	0.112706E+20
140.00	206.202	0.270678E+19	0.139774E+20
150.00	209.285	0.358291E+19	0.175603E+20
160.00	212.186	0.465471E+19	0.222150E+20
170.00	215.180	0.594897E+19	0.281640E+20
180.00	218.003	0.749409E+19	0.356581E+20
190.00	220.673	0.932014E+19	0.449782E+20
200.00	223.206	0.114588E+20	0.564370E+20
220.00	227.846	0.306525E+20	0.870895E+20
240.00	231.974	0.438028E+20	0.130892E+21
260.00	235.771	0.607579E+20	0.191650E+21
280.00	239.735	0.821791E+20	0.273829E+21
300.00	243.597	0.108779E+21	0.382608E+21
320.00	247.210	0.141319E+21	0.523927E+21
340.00	250.602	0.180613E+21	0.704540E+21
360.00	253.800	0.227524E+21	0.932064E+21
380.00	256.825	0.282963E+21	0.121503E+22
400.00	259.695	0.347894E+21	0.156292E+22
425.00	263.086	0.541933E+21	0.210485E+22
450.00	265.959	0.682689E+21	0.278754E+22
475.00	268.674	0.849036E+21	0.363658E+22
500.00	271.250	0.104386E+22	0.468044E+22
525.00	273.701	0.127020E+22	0.595064E+22
550.00	276.098	0.153123E+22	0.748187E+22
575.00	278.410	0.183029E+22	0.931216E+22
600.00	280.623	0.234674E+22	0.116589E+23
625.00	282.745	0.292633E+22	0.145852E+23
650.00	284.784	0.356968E+22	0.181549E+23
675.00	286.746	0.427707E+22	0.224320E+23
700.00	288.637	0.504860E+22	0.274806E+23
725.00	290.462	0.588423E+22	0.333648E+23
750.00	292.477	0.671308E+22	0.400779E+23
775.00	295.196	0.727340E+22	0.473513E+23
800.00	297.829	0.756085E+22	0.549121E+23
825.00	300.381	0.775532E+22	0.626675E+23
850.00	302.856	0.784346E+22	0.705109E+23
875.00	305.260	0.781247E+22	0.783234E+23
900.00	307.596	0.764972E+22	0.859731E+23
925.00	309.744	0.761635E+22	0.935895E+23
950.00	311.815	0.779832E+22	0.101388E+24
975.00	313.833	0.797453E+22	0.109362E+24
1000.00	315.800	0.810376E+22	0.117466E+24

intervals of: (1) less than 200 mb, (2) 200-300 mb, (3) 300-500 mb, (4) 500-700 mb, and (5) 700-1000 mb. A sixth layer value (less than 1000 mb) was defined to provide the total integrated water vapor column. For each of the dependent sets of atmospheres, layer water vapor statistics were evaluated to provide a climatology for retrieval comparison purposes. These statistics are given in Table 2-3 and include layer mean values, standard deviations and fractional RMS variabilities (may be expressed as percent by multiplying by 100). The RMS values can be considered as a measure of the climatological variation of layer water vapor column densities for each set of atmospheres against which to measure a given retrieval method. They are plotted in Figure 2-8. For example, if the mean water vapor density for each layer were chosen as a first-guess retrieved value, the RMS error of the method evaluated over the set would be the variability shown in Figure 2-8. While the properties of the climatologies illustrated are generally reasonable (i.e. least variability near the surface for tropical case over the ocean and most for midlatitude winter cases), the decrease of variability at higher levels is most likely an artifact of filling missing upper level values in the original incomplete soundings with climatology.

2.4.2   Simulation Results

Rapid algorithm AMTS water vapor channel simulations were performed using the selected sounding sample sets described above in order to investigate relationships between resultant channel brightness temperatures, atmospheric transmittances, and water vapor profile. Brightness temperatures were calculated for each dependent sounding set without adding instrumental noise. The results of these simulations were used to generate scatter diagrams to test a few basic hypotheses. Early in the course of the simulation modeling it was observed that the calculated i^{th} channel transmittance to space, τ^i, from the pressure level in the model atmosphere with local physical temperature, $T(p)$, equal to the simulated channel brightness temperature, T_b^i, was approximately constant, i.e.:

$$\tau^i[p(T = T_b^i)] \approx const \qquad (2.2)$$

This constant was ~0.50 for channels not affected by surface contributions or the tropopause. Figure 2-9, for example, illustrates a scatter plot of T_b^i vs.

Table 2-3

Means, Standard Deviations, and RMS Variability of Layer
Water Vapor Abundances for Atmospheric Sample Dependent Sets

Atmosphere Sample	Layer	Pressure Range (mb)	Mean	SDEV	RMS
Tropical Winter	1	< 200	0.5737E+20	0.1182E+20	0.2050E+00
	2	200-300	0.3492E+21	0.1414E+21	0.4030E+00
	3	300-500	0.5039E+22	0.2926E+22	0.5777E+00
	4	500-7000	0.2198E+23	0.1263E+23	0.5715E+00
	5	700-1000	0.9198E+23	0.3047E+23	0.3296E+00
	6	< 1000	0.1194E+24	0.4352E+23	0.3626E+00
Midlatitude Winter	1	< 200	0.4341E+20	0.8663E+19	0.1985E+00
	2	200-300	0.1954E+21	0.8361E+20	0.4257E+00
	3	300-500	0.2133E+22	0.1355E+22	0.6320E+00
	4	500-700	0.8421E+22	0.5714E+22	0.6751E+00
	5	700-1000	0.3438E+23	0.1914E+23	0.5541E+00
	6	< 1000	0.4517E+23	0.2382E+23	0.5247E+00
Tropical Summer	1	< 200	0.4882E+20	0.1029E+20	0.2095E+00
	2	200-300	0.2519E+21	0.1125E+21	0.4445E+00
	3	300-500	0.3128E+22	0.2112E+22	0.6718E+00
	4	500-700	0.1288E+23	0.8734E+22	0.6746E+00
	5	700-1000	0.6894E+23	0.3185E+23	0.4596E+00
	6	< 1000	0.8526E+23	0.4018E+23	0.4690E+00
Midlatitude Summer	1	< 200	0.5115E+20	0.9153E+19	0.1780E+00
	2	200-300	0.2739E+21	0.1049E+21	0.3811E+00
	3	300-500	0.3481E+22	0.2053E+22	0.5869E+00
	4	500-700	0.1483E+23	0.8675E+22	0.5816E+00
	5	700-1000	0.6772E+23	0.2612E+23	0.3838E+00
	6	< 1000	0.8636E+23	0.3419E+23	0.3938E+00
Tropical Winter (ocean only)	1	< 200	0.5588E+20	0.1068E+20	0.1901E+00
	2	200-300	0.3295E+21	0.1272E+21	0.3842E+00
	3	300-500	0.4594E+22	0.2613E+22	0.5658E+00
	4	500-700	0.2044E+23	0.1188E+23	0.5785E+00
	5	700-1000	0.1013E+24	0.2884E+23	0.2833E+00
	6	< 1000	0.1267E+24	0.4018E+23	0.3155E+00

RMS

0.20　0.40　0.60　0.80

CLIMATOLOGY

0.00

200.00

400.00

600.00

800.00

AVG. PRESSURE (MB)

⊙ TROPICAL WINTER
△ TROPICAL SUMMER
+ MIDLATITUDE WINTER
X MIDLATITUDE SUMMER
◇ TROP. WINTER (OCEAN ONLY)

0.20　0.40　0.60　0.80

0.00　200.00　400.00　600.00　800.00

AVG. PRESSURE (MB)
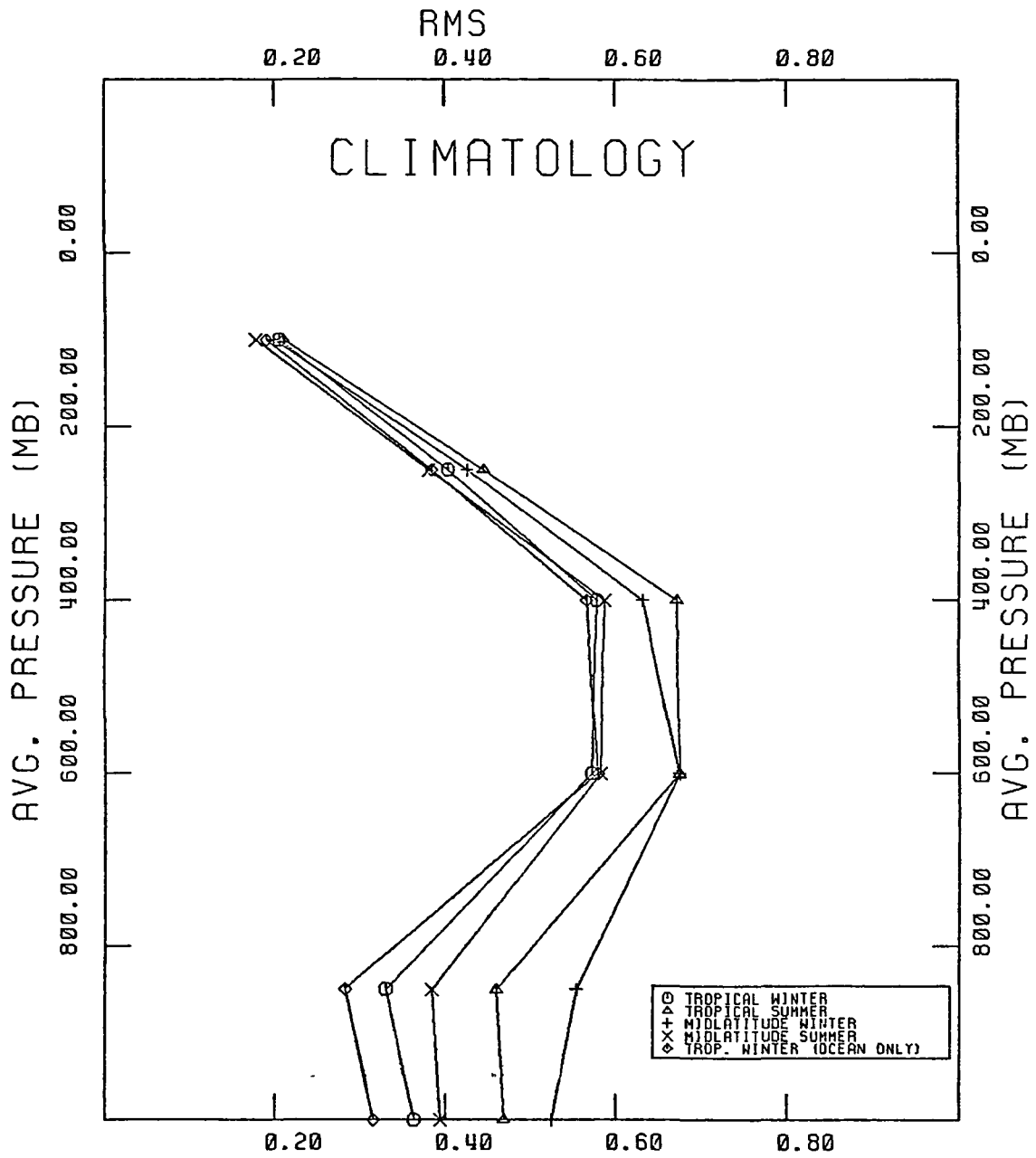
Figure 2-8. RMS Variability of Atmospheric Sample Dependent Sets
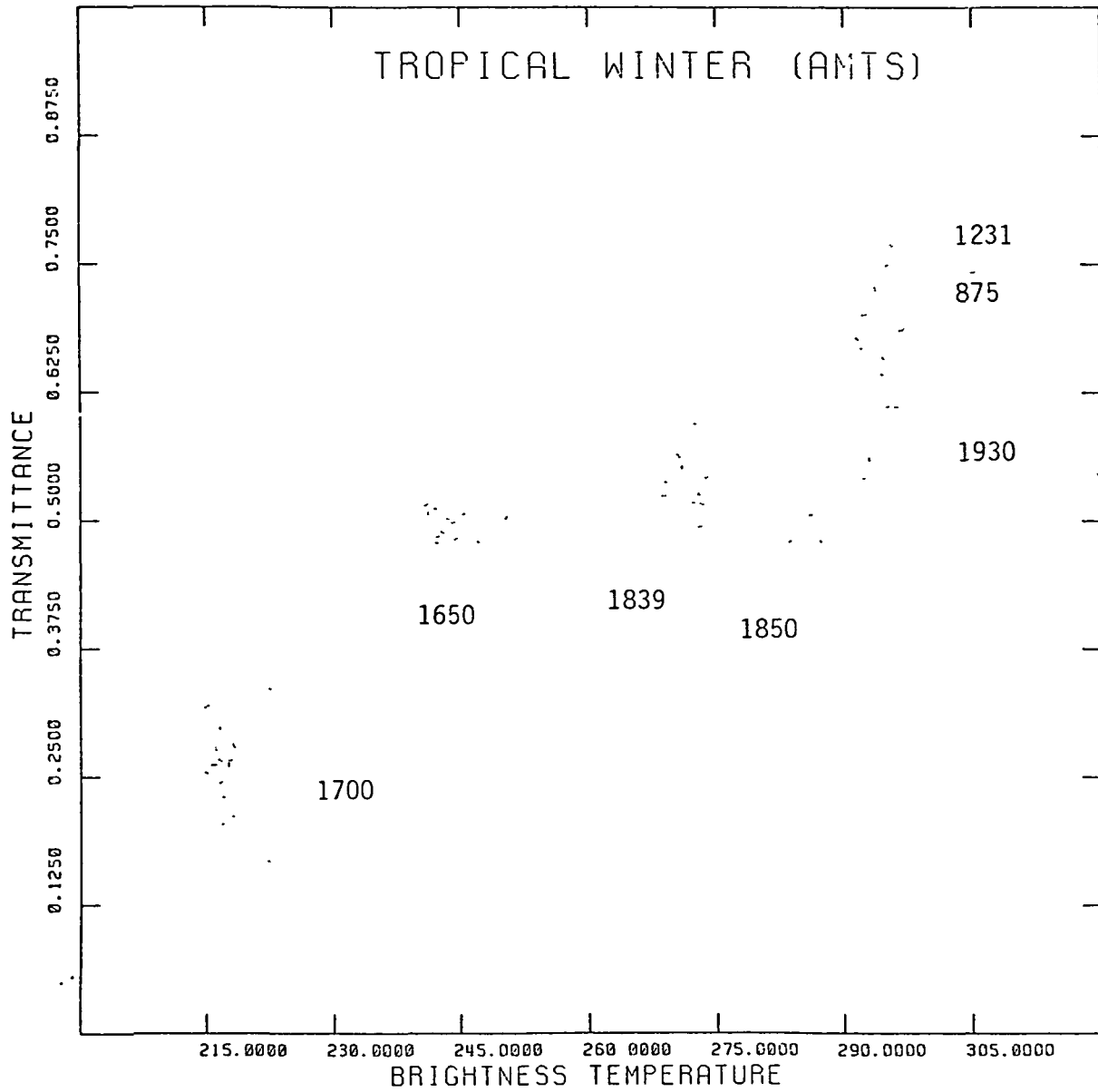
Figure 2-9. Simulated AMTS channel transmittance vs. brightness
temperature for dependent tropical winter (over
ocean only) atmospheres.

τ^i for the five AMTS water vapor channels (1700.3, 1650.1, 1839.4, 1850.9, 1930.1 cm^{-1}) and two surface channels (875.0, 1231.8 cm^{-1}) calculated for the TW (ocean only) set of soundings. The pressure level, $p(T = T_b^i)$, for each channel, i, was identified for each sounding using the corresponding temperature profile assumed as known. Note that with the exception of points near temperatures of about 215 K and 290 K due to the exception noted above (from the 1700 cm^{-1} and 875, 1231.8 cm^{-1} channels, respectively), most channels whose weighting functions peak in mid-atmosphere cluster about $\tau \approx$ 0.50.

This observation led to exploring the relationship between channel brightness temperature T_b^i, and integrated water vapor column density to the level $U_i[cm^{-2}]$ defined as:

$$U_i[p(T = T_b^i)] = \int_p^0 n(p) \, H(p) \, d\ln p \qquad (2.3)$$

where $n[cm^{-3}]$ is the local water vapor number density and $H[cm]$ is the local scale height. This relationship is illustrated in Figure 2-10. Notably, each water vapor channel corresponds to a relatively fixed integrated column density (with some channels exhibiting an apparently linear dependence on T_b^i). As expected, the magnitude of the integrated water vapor column sensed by each channel increases as the peak of its characteristic weighting function approaches the surface (cf. Figure 2-1). The surface channels are clustered in the upper right hand corner. This observation suggests that a first order profile may be constructed by assigning a channel specific integrated column water vapor amount to a pressure level defined by the channel brightness temperature and a knowledge of the temperature profile.

An analogous set of scatter diagrams was generated for the three water vapor channels (1484.4, 1363.7, 1217.1 cm^{-1}) and window channel (897.7 cm^{-1}) of the TOVS HIRS-2 sounder. These are illustrated in Figures 2-11 and 2-12, respectively. Intercomparison with the previous two figures indicate relationships with behavior which is quantitatively similar to that noted for the AMTS. Most differences between the AMTS and HIRS results are likely due to the number of channels and spacing of integrated water vapor column amounts sensed by each instrument's channel set. For example, the AMTS has more water vapor channels including one (at 1700 cm^{-1}) which senses a column about a factor of ten less (i.e., higher in the atmosphere) than the highest HIRS channel (at 1484 cm^{-1}).
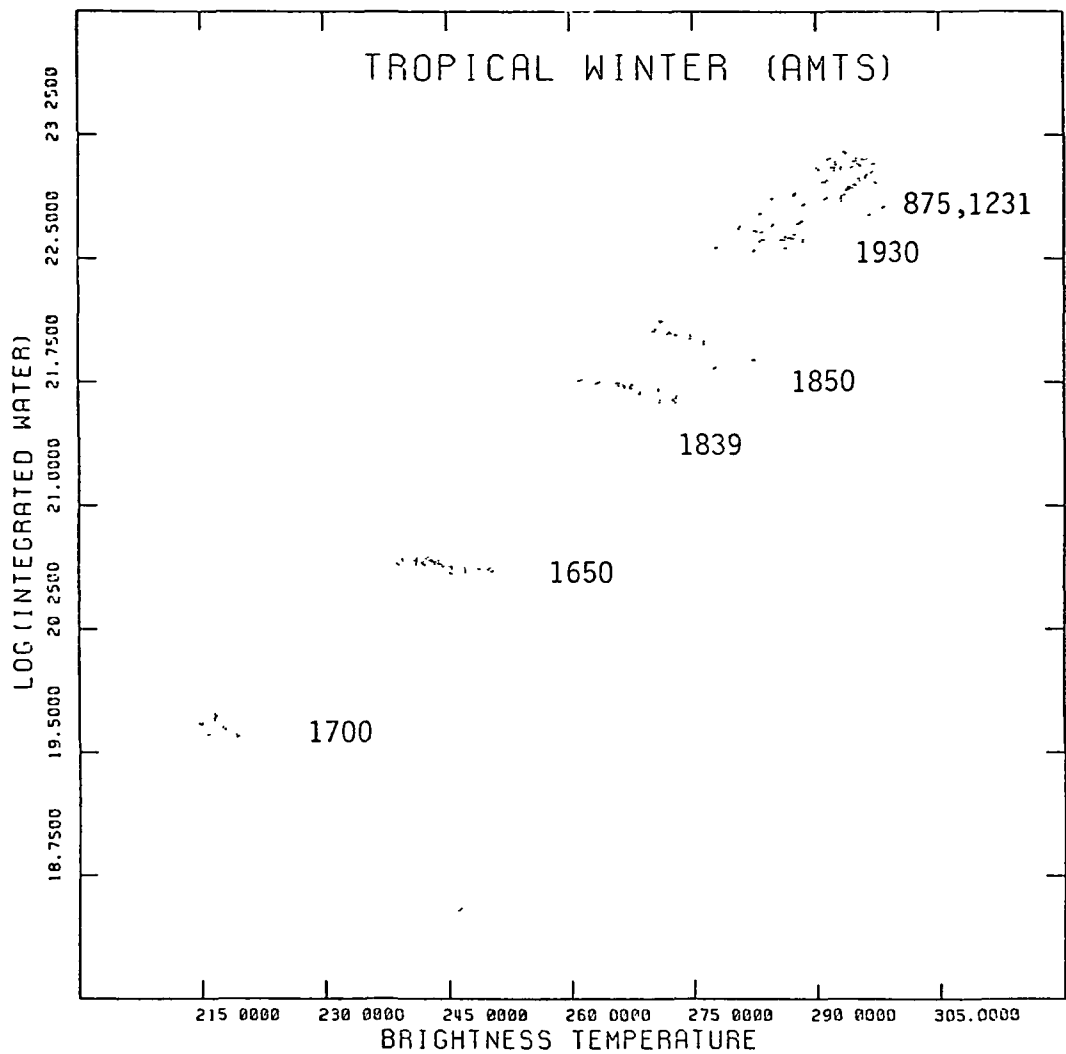
Figure 2-10. Simulated AMTS channel brightness temperature vs. integrated water vapor for dependent tropical winter (over oceans only) atmospheres.
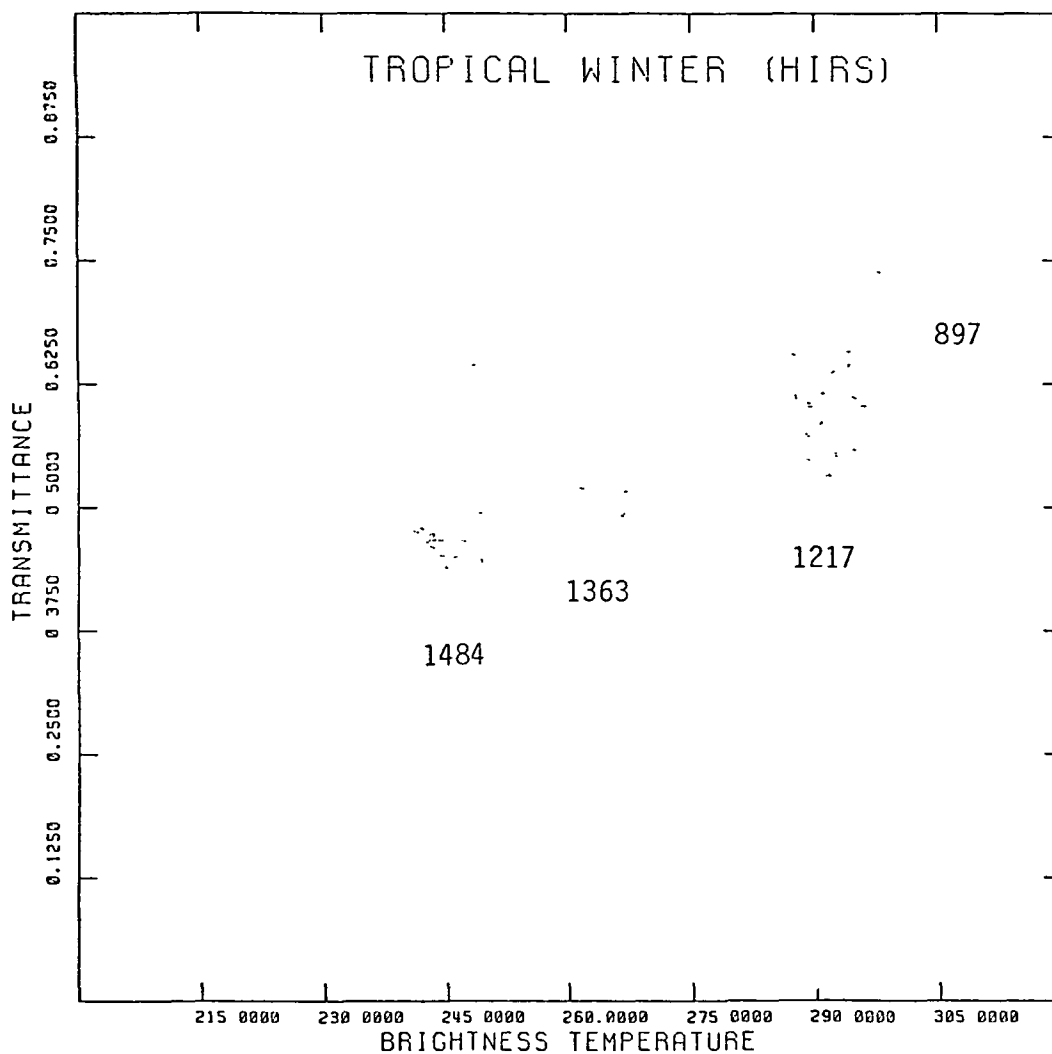
Figure 2-11. Simulated HIRS channel transmittance vs. brightness
              temperature for dependent tropical winter (over
              ocean-only) atmospheres
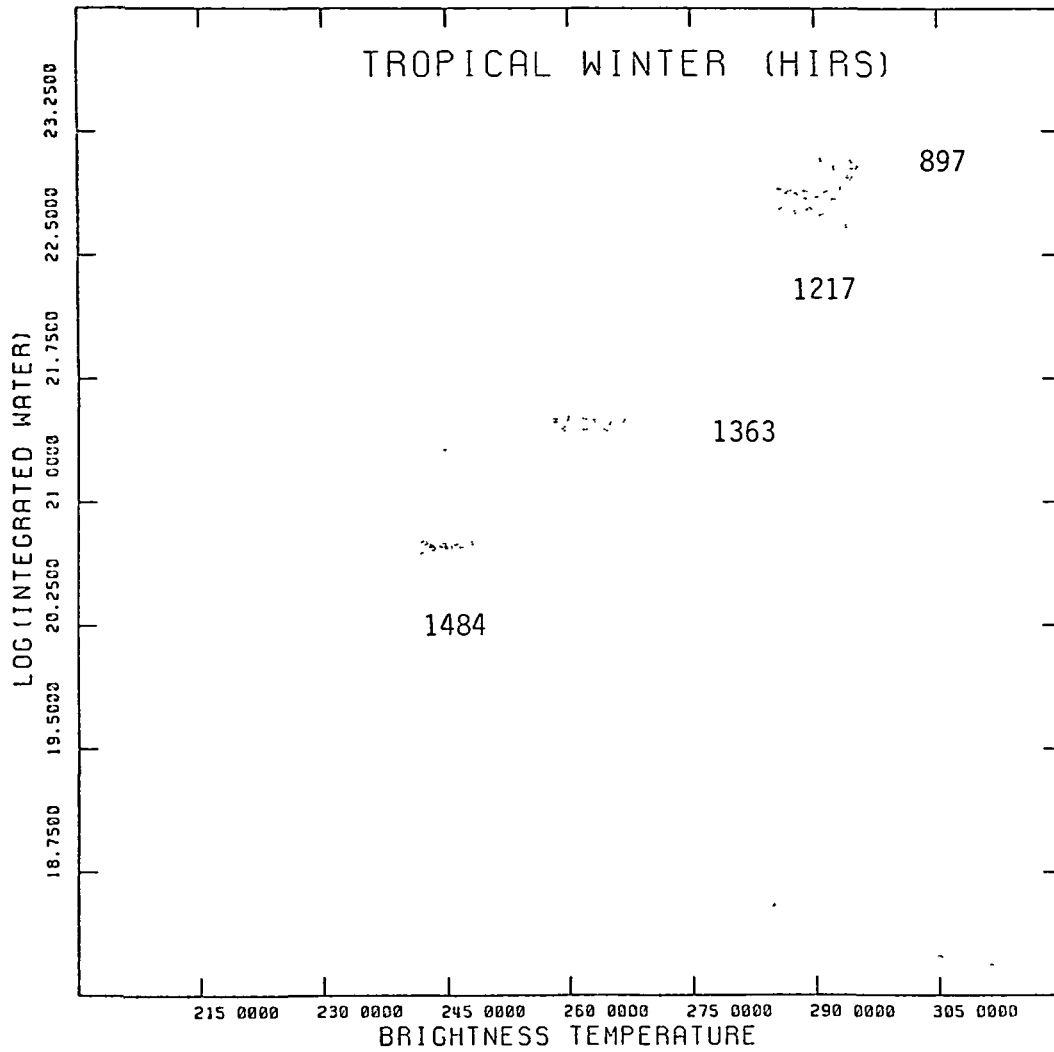
Figure 2-12. Simulated HIRS channel brightness temperature
vs. integrated water vapor for dependent tropical
winter (over oceans only) atmospheres.

The success of the first order approach described above will depend to a great extent on how invariant the specific integrated column water vapor amount is for each channel. Figure 2-13 illustrates the AMTS brightness temperature integrated water scatter diagrams analogous to Figure 2-10 above for each of the sample atmospheric profile sets. Qualitatively, it is notable that when these four plots are superimposed, channels cluster for the most part in their own characteristic domains, i.e. the association of an integrated column for each channel is only weakly dependent on season and latitude. Exceptions are largely attributable to surface effects. It is notable, however, that the individual scatter diagrams differ in detail. Specifically, the separation notable for individual channel brightness temperature/integrated water curves of the TW (ocean only) set (Figure 2-10) and the TW set presented here (Figure 2-13b), becomes somewhat less distinct for the channels affected by the lower atmosphere and surface (upper right hand corner of each scatter diagram). This is particularly evident for the midlatitude winter results (Figure 2-13d) where the lowest three water vapor channels (1839, 1850, 1930) and surface channels (875, 1231) tend to blend together. Additionally, the remarkable "bullet" pattern noted for the highest peaking channel at 1700 cm^{-1} (in the lower left hand corner of each scatter diagram) is destroyed in going from tropical (Figure 2-13a,b) to midlatitude soundings (Figure 2-13c,d). This is likely due to differences in variances of the height of the tropopause.
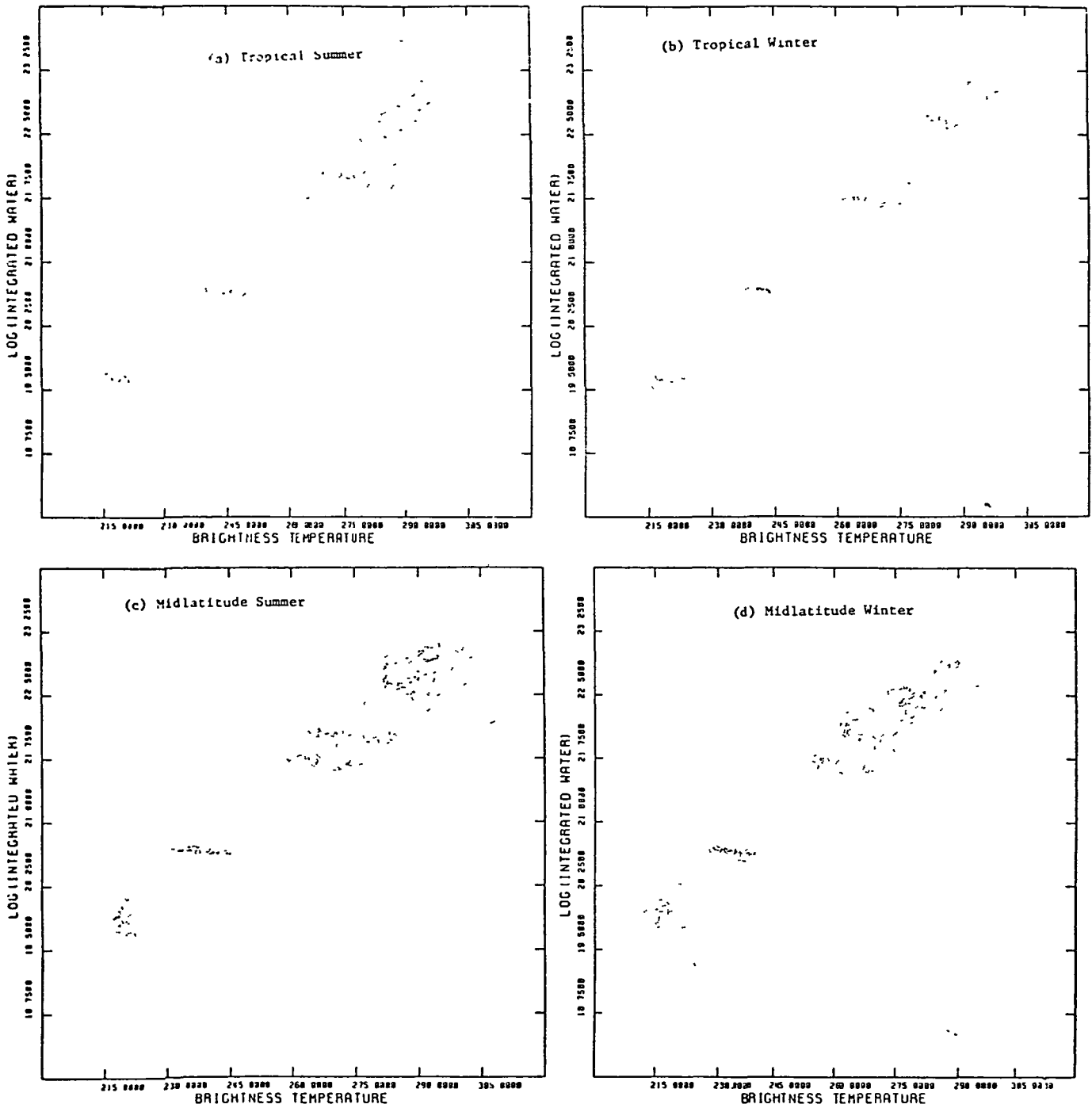
Figure 2-13. Results of brightness temperature simulations for dependent sets of atmospheric profiles: (a) Tropical Summer, (b) Tropical Winter, (c) Midlatitude Summer, and (d) Midlatitude Winter.

-29-

3. DEVELOPMENT OF A FIRST GUESS RETRIEVAL ALGORITHM

3.1 Background

The brightness temperature simulation results described in the previous section (§2.4.2) suggest that to first order, each AMTS water vapor channel senses an essentially constant column of water vapor related to an approximately constant value of transmittance or, alternatively, optical depth. This notion is conceptually supported by the water vapor channel weighting functions calculated as functions of integrated column density (Equation 2.1) illustrated in Figure 2-4. Furthermore, the pressure level corresponding to this integrated column is approximately that for which the local temperature is equal to the channel's brightness temperature. Thus, given a knowledge of both the temperature profile, $T(p)$ (from a temperature retrieval, for example) and the water vapor channel brightness temperatures, it should be possible to infer the vertical distribution of water vapor by assigning the specified column amount for each channel, U_i, to that pressure level described above, i.e.,

$$U \left[p(T = T_b^i) \right] = U_i \tag{3.1}$$

and producing a smooth profile by interpolation. In practice, problems are introduced by a variety of necessary operations including: (1) determining an integrated column amount to assign to each channel, (2) interpolating between pressure levels both to produce a smooth integrated column profile and provide layer amounts for specified pressure level boundaries from column amounts, (3) extrapolating above the lowest pressure level and below the highest pressure level (the latter occasionally leading to supersaturation in the surface layer), and (4) assigning a pressure level to each channel for a given retrieval due to errors in the associated temperature profile.

In this section, the development of a novel first guess water vapor profile retrieval algorithm based on the above hypothesis is described. Figure 3-1 illustrates a schematic of the first guess retrieval algorithm. The retrieved layer values are obtained from synthetic noisy water vapor channel brightness temperature data obtained from the independent sets of atmospheric soundings (see 2.4.1) using the rapid algorithm. The method is tested and verified by comparing retrieved layer values with those of the
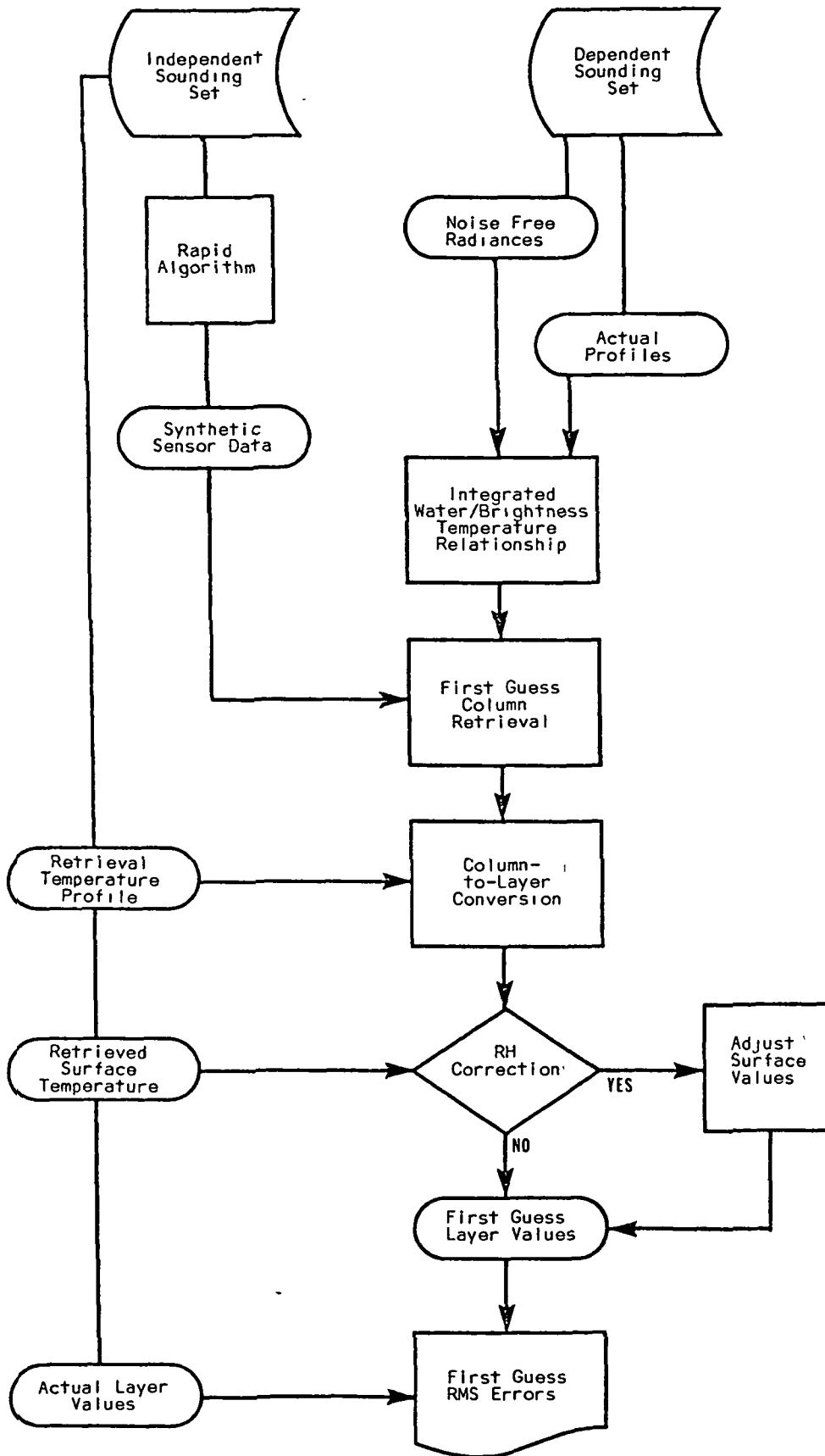
Figure 3-1. Schematic of First Guess Retrieval Algorithm

actual soundings and evaluating RMS error statistics over the entire ensemble of soundings. Possible solutions to the problems enumerated above are also described.

3.2 First Guess Retrieval of Integrated Column Amounts

A basic consideration is the selection of a reasonable method to assign a column integrated water vapor amount to each AMTS channel based on the brightness temperature simulation results for the dependent sounding sets illustrated in Figure 2-13. Three candidate approaches were investigated using: (a) the mean value of the column integrated water vapor for each channel, (b) a linear fit of the log of the column integrated water vapor, U_i, for the ith channel with the channel brightness temperature T_b^i of the form

$$\log U_i = a_i T_b^i + b_i \qquad (3.2)$$

and (c) a multiple regression equation based on the channel brightness temperature and other presumed known parameters (such as the height of the tropopause). Each method was evaluated by applying the selected channel specific values to retrieve integrated column amounts for each channel using noisy synthetic brightness temperatures calculated for the independent set and examining the resulting RMS error. The RMS error for the ith channel integrated column amount evaluated over the set of N = 100 independent soundings was defined as:

$$RMS(i) = \frac{1}{\bar{U}(i)} \left\{ N^{-1} \sum_{j=1}^{N} \left[\hat{U}(i,j) - U(i,j) \right]^2 \right\}^{1/2} \qquad (3.3)$$

where $\hat{U}(i,j)$ and $U(i,j)$ are, respectively, the retrieved and actual column integrated water vapor amounts for the ith channel and j^{th} sounding and $\bar{U}(i)$ is the channel mean value. It is important to note that the quantities being retrieved here, the $\hat{U}(i,j)$, are not referenced to a fixed pressure level since even for a given channel, this will vary among the soundings with the vertical distribution of water vapor and temperature. This is simply a test of the potential for using the results of the forward problem to infer the column values sensed by each channel. The sources of error were the channel-dependent instrumental noise introduced in the generation of synthetic brightness temperature, 1.5 K of assumed temperature retrieval

uncertainty, and the choice of method assumed above. Results are given in Table 3-1 for the tropical winter set of soundings corresponding to Figure 2-13b. For channels not influenced by the surface and upper atmosphere, the simple linear fit appears to perform adequately. As might be expected, channels with distinct linear patterns in the scatter diagram (e.g., 1650.1 cm^{-1}) produce the best retrievals, while those influenced by the surface (875.0, 1231.8 cm^{-1}) are least accurate.

Applying the linear fit approach to the dependent sounding set simulations illustrated in Figure 2-13 results in the regression and correlation coefficients summarized in Table 3-2. These regression coefficients are subsequently used as the basis for retrieving channel integrated water vapor values from synthetic channel brightness temperature data generated from the independent set of soundings. Some measure of the potential success of this approach is provided by the individual channel correlation coefficients which should be greater than about 0.4 for this sample size to suggest statistically significant linear dependence.

3.3 First Guess Retrieval of Layer Amounts

Using the approach described above, each channel associates a column water vapor amount with a pressure level. Using the water vapor channels and one surface channel, for example, six points along the integrated water vapor profile are determined. The pressure levels associated with these points vary with each sounding, however, and therfore it is convenient to provide for calculating a continuous profile. This also facilitates retrieving layer amounts within fixed pressure increments.

A piecewise smooth integrated column profile is evaluated using segments individually fit as:

$$U(p) = U(p_{j+1}) \left(p/p_{j+1}\right)^{\lambda_j} \text{ for } p_j \leqslant p \leqslant p_{j+i} . \tag{3.4}$$

where the power law experiment λ_j is given for each segment by:

$$\lambda_j = \frac{\ln[U(p_j)/U(p_{j+1})]}{\ln(p_j/p_{j+1})} \tag{3.5}$$

Values are extrapolated above the lowest pressure value (for the 1700 cm^{-1}) and to the surface.

Table 3-1

Effect of Channel/Column Amount Assignment Method on
RMS Errors for Retrieval of Level Integrated
Water Vapor Column Amounts for Tropical Winter Soundings

Channel	Means	Linear	Multiple
1650.1	.0601	.0468	.0468
1700.3	.1796	.1803	.3339
1839.4	.1046	.08941	.08941
1850.9	.1614	.1543	.1543
1930.1	.1809	.1642	.2304
875.0	.2329	.2367	.2516
1231.8	.2687	.2842	.2961

Table 3-2

Means, Standard Deviations, and RMS Variability of Layer
Water Vapor Abundances for Atmospheric Sample Dependent Sets

Atmosphere Sample	AMTS Channel	Regression Coefficients a_i	b_i	Correlation Coefficient
Tropical Winter	1650.1	-.682894E-02	0.223116E+02	0.698516E+00
	1700.3	-.207474E-02	0.201019E+02	0.740448E+00
	1839.4	-.881106E-02	0.240791E+02	0.662491E+00
	1850.9	-.127429E-01	0.255050E+02	0.609532E+00
	1930.1	-.115886E-01	0.259446E+02	0.564673E+00
	875.0	-.104205E-01	0.260061E+02	0.418703E+00
	1231.8	-.971928E-02	0.258259E+02	0.316401E+00
Midlatitude Winter	1650.1	-.794979E-02	0.225060E+02	0.647118E+Q0
	1700.3	-.641433E-02	0.213317E+02	0.921094E+01
	1839.4	-.399605E-02	0.227093E+02	0.149386E+00
	1850.9	-.359382E-02	0.229308E+02	0.113795E+00
	1930.1	0.210679E-01	0.165564E+02	0.675599E+00
	875.0	0.255938E-01	0.153525E+02	0.771720E+00
	1231.8	0.237758E-01	0.158645E+02	0.764807E+00
Tropical Summer	1650.1	-.680776E-02	0.222915E+02	0.644311E+00
	1700.3	-.987208E-02	0.218247E+02	0.335425E+00
	1839.4	-.996337E-02	0.243636E+02	0.556745E+00
	1850.9	-.139610E-01	0.258160E+02	0.472715E+00
	1930.1	-.101513E-01	0.254136E+02	0.205299E+00
	875.0	0.280548E-01	0.145925E+02	0.463431E+00
	1231.8	0.310113E-01	0.137363E+02	0.518697E+00
Midlatitude Summer	1650.1	-.483858E-02	0.218171E+02	0.663063E+00
	1700.3	-.151727E-01	0.232295E+02	0.141038E+00
	1839.4	-.496142E-02	0.230231E+02	0.468682E+00
	1850.9	-.798210E-02	0.241753E+02	0.513617E+00
	1930.1	-.658089E-02	0.243887E+02	0.205369E+00
	875.0	0.138860E-01	0.187229E+02	0.374975E+00
	1231.8	0.159077E-01	0.181412E+02	0.430633E+00

Results of the first guess algorithm using AMTS and the three integrated column amount selection methods described in the previous section are shown in Figure 3-2. Layer water vapor column accounts (cm^{-2}) were retrieved from the independent set of TW atmospheres using regression coefficients (Table 3-2) derived from the dependent set (Figure 2-13b). In determining pressure levels for each channel, temperature retrieval error of 1.5 K was assumed at all levels. RMS percent errors were evaluated for five retrieval layers corresponding to: (a) 0-200 mb, (b) 200-300 mb, (c) 300-500 mb, (d) 500-700 mb, and (e) 700-1000 mb, and are plotted at each layer's average pressure. These layers were chosen both to correspond to lower atmospheric pressure level increments used in the reporting of the operational water vapor products supported by the HIRS-2 sensor (Smith et al., 1979; NOAA, 1981) and to explore the potential for increased vertical resolution in the upper atmosphere from the AMTS. The points plotted at 1000 mb correspond to the RMS errors of the total integrated water vapor column. The RMS error for each layer k evaluated over the set of N = 100 independent soundings was defined as:

$$RMS(k) = \frac{1}{\bar{u}(k)} \left\{ N^{-1} \sum_{j=1}^{N} \left[\hat{u}(k,j) - u(k,j) \right]^2 \right\}^{1/2} \qquad (3.6)$$

where $\hat{u}(k,j)$ and $u(k,j)$ are, respectively, the retrieved and actual water vapor amounts for the kth layer and j^{th} sounding and $\bar{u}(k)$ is the layer mean value.

For comparison purposes, the RMS variation of the dependent set of atmospheres is also shown as climatology. The algorithm appears to provide a reasonable first guess water vapor profile based on improvement over climatology throughout most of the atmosphere.

Comparing the three column amount selection methods, both the mean and linear fit appear to be equally applicable. The latter was retained to perform subsequent calculations. Problems are evident in retrieving the surface layer (plotted at 850 mb) and that above 200 mb (plotted at 100 mb). An important source of error introduced in the process of retrieving layer values is that due to the power law interpolation method and subsequent extrapolation, especially to the surface. This is in addition to the effects of instrumental noise and errors in the retrieved temperature profile. These factors are discussed in the sections to follow.
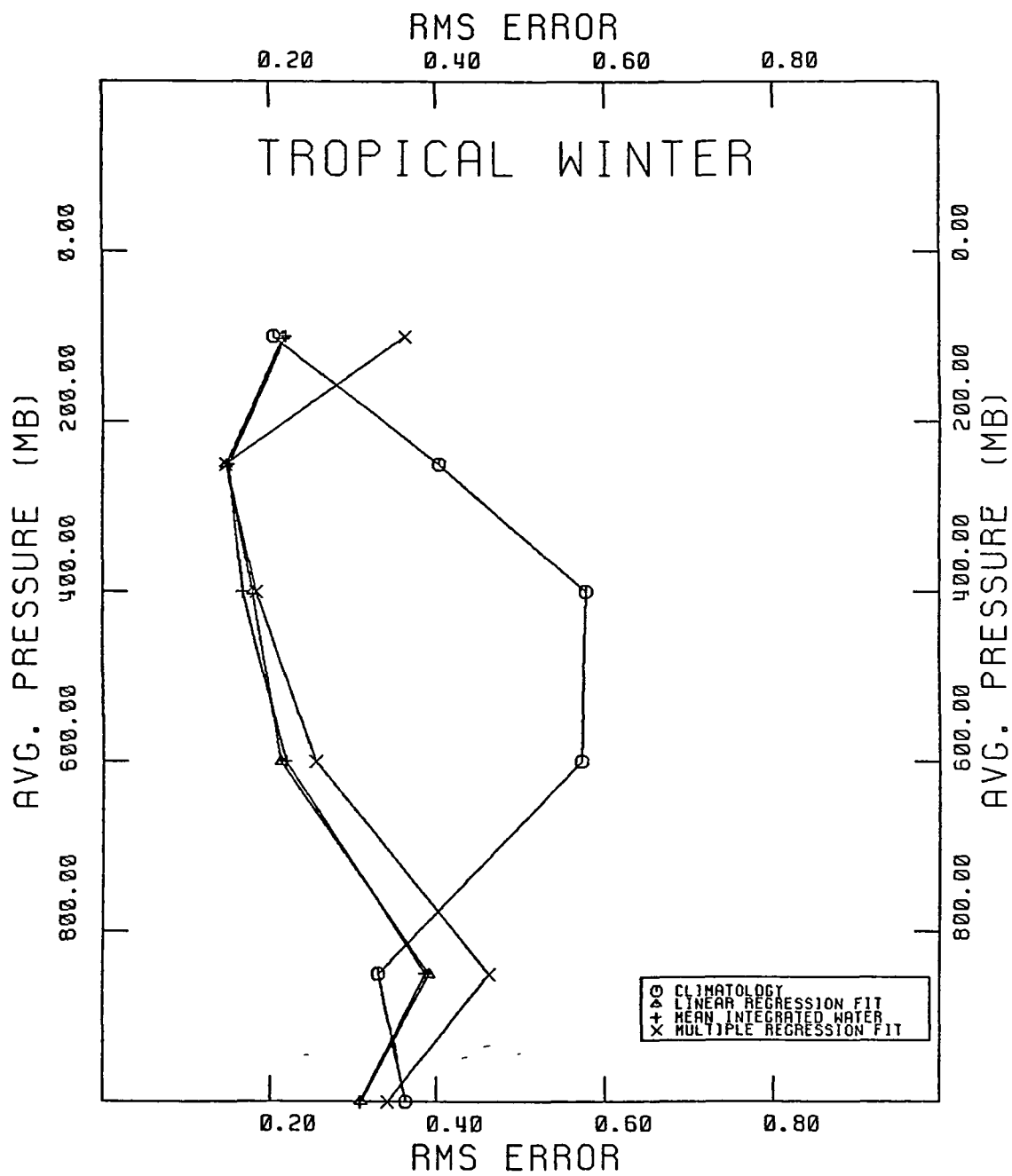
Figure 3-2. Comparison of RMS errors of first guess layer water vapor
values to climatology for tropical winter atmospheres retrieved
using: linear fit, channel mean values, and multiple regression.

It should be noted that the data set was extrapolated from 300 mb or greater pressure to climatological mean values at 100 mb. These and subsequent results, therefore, are unfortunately not helpful in testing the usefulness of the 1700 cm^{-1} channel.

3.4 Errors Due to Power Law Smoothing

The numerical device of power law smoothing of the retrieved integrated column water vapor amounts between pressure levels and extrapolation beyond this domain introduces some error in the first guess procedure. From Table 3-1, for example, it may be noted that RMS errors in retrieving integrated column amounts near the surface for the TW sample set using the linear fit method are between 16 and 29% using the 1930.1 and 1231.8 cm^{-1} channels, respectively. In Figure 3-2, however, retrieval accuracy for the layer nearest the surface (i.e. 700-1000 mb) is reduced to about 40%. To isolate the errors due to smoothing (both interpolation and extrapolation) on first guess retrieval errors, the exact column amounts from the independent TW set were input as retrieved values to the layer fitting scheme and RMS errors of the resultant layer values were calculated. Additionally, to eliminate temperature error effects the exact temperature profiles were used for each sounding (i.e., 0.0 K temperature error). The results are shown in Figure 3-3. (In this and subsequent like figures the first guess curve refers to a linear fit.) While there is a small amount of RMS error introduced in the highest layer retrieval (< 200 mb) due to extrapolation, most of the effect is apparent in the lowest two layers (i.e. 500-700 mb, 700-1000). The middle two layers (i.e. 200-300 mb, 300-500 mb) are hardly affected. The magnitude of the RMS error due to extrapolation to the surface for the lowest layer is about 10%. As will be discussed in Section 3.6, much of this error is attributable to soundings with relatively dry layers at the surface.

3.5 Errors Due to Uncertainties in the Temperature Profile

The first guess procedure for each water vapor channel is based on identifying that pressure level within a given sounding where the brightness temperature is equal to the actual level temperature. Since retrieved temperature profiles must be used to accomplish this in practice, their associated errors critically constrain the potential accuracy of the first guess moisture retrieval process. This is illustrated by a second curve in
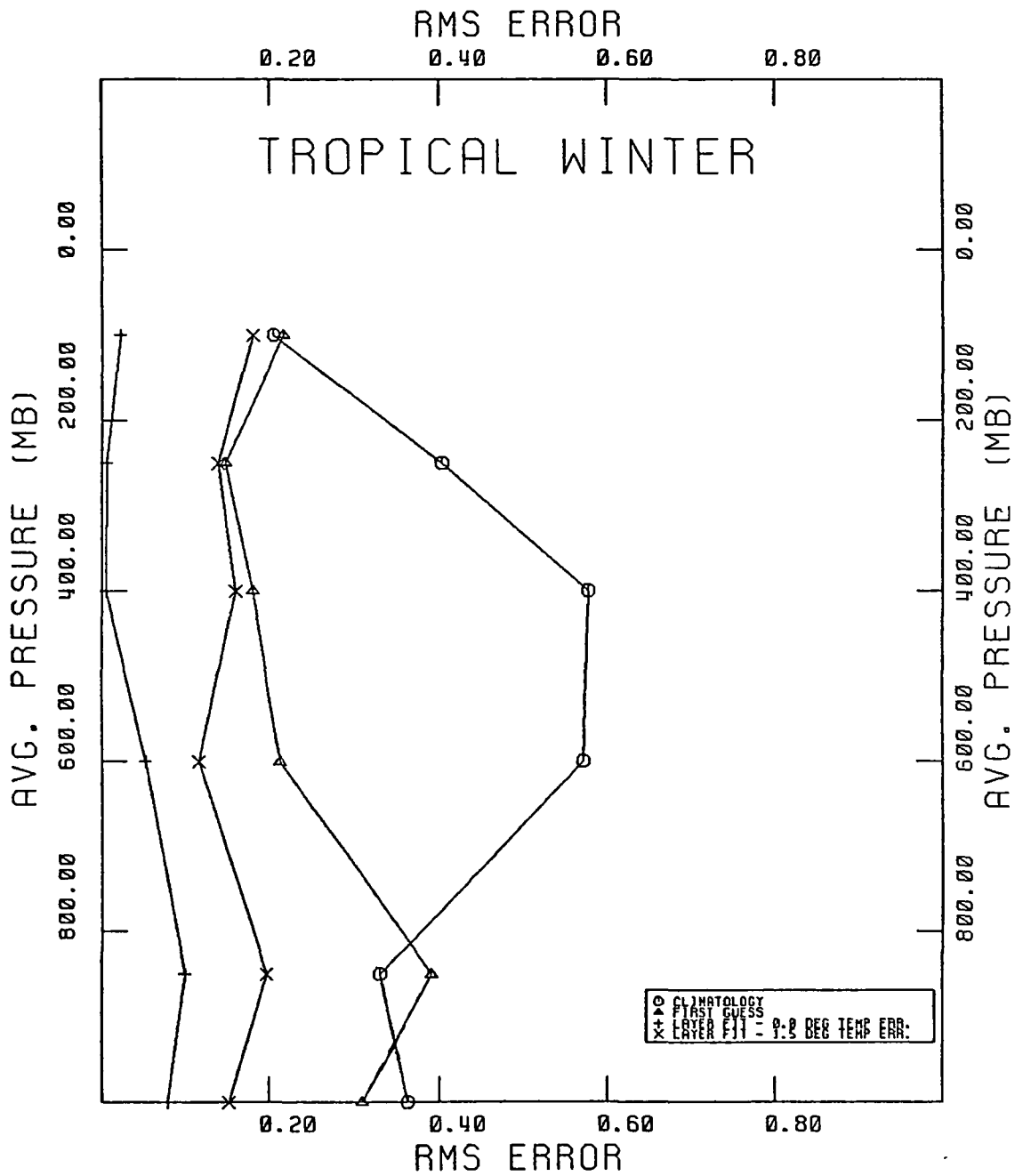
Figure 3-3. RMS errors of first guess layer water vapor values for tropical winter atmospheres retrieved using: true integrated column amounts and temperature profiles, true integrated column amounts and simulated temperature profile errors of 1.5 K, and simulated integrated column amounts and temperature profiles (i.e. first guess).

Figure 3-3 derived by repeating the calculation discussed in the previous section, however, now including a temperature profile retrieval error of 1.5 K.

Comparing this curve to the previous results (no error in column amounts or temperature profiles) and to the first guess curve (errors in both column amounts and temperature profiles), it can be observed that in the upper three layers, much if not all of the RMS error in the water vapor retrieval is due to uncertainties associated with the temperature retrieval. In the lowest layer about a quarter of the error each is attributable to extrapolation and temperature error while about half is due to uncertainties in obtaining the water vapor amounts themselves. In the remaining layer (centered at 600 mb), these factors contribute about one third each to the RMS error.

3.6 Corrections for Supersaturation in the Surface Layer

An examination of individual water vapor soundings within the TW set indicated that surface layer values were occasionally quite overestimated by the first guess retrieval due to extrapolation of the column profile to the surface (as noted in Section 3.4). In order to circumvent this situation where possible, a method was developed to test the near surface layer in each first guess retrieval for supersaturation (i.e. relative humidity of greater than 100%) and correct if necessary by reducing the layer water vapor amount accordingly. The algorithm calculates relative humidity from the water vapor amount given by the first guess profile in the lowest layer between 975 and 1000 mb and an assumed surface temperature, T_s. If this layer is supersaturated the power law exponent in the fit for the lowest surface layer is reduced to bring the relative humidity to a value less than 100%. Conceptually, the surface temperatures should be available from one of the AMTS super window channels to an accuracy of about 1.5 K (Chahine et al., 1984).

The results of testing the surface layer correction are shown in Figure 3-4. The previous first guess results with no relative humidity correction are included for comparison. Four cases were considered corresponding to: (1) assuming a constant value for the surface temperature (300 K), and retrieving surface temperature with errors of (2) 0.0 K, (3) 1.5 K, and (4) 2.0 K, respectively. The retrieved surface temperatures were the actual 1000 mb temperatures with an added random error. Correcting for supersaturation
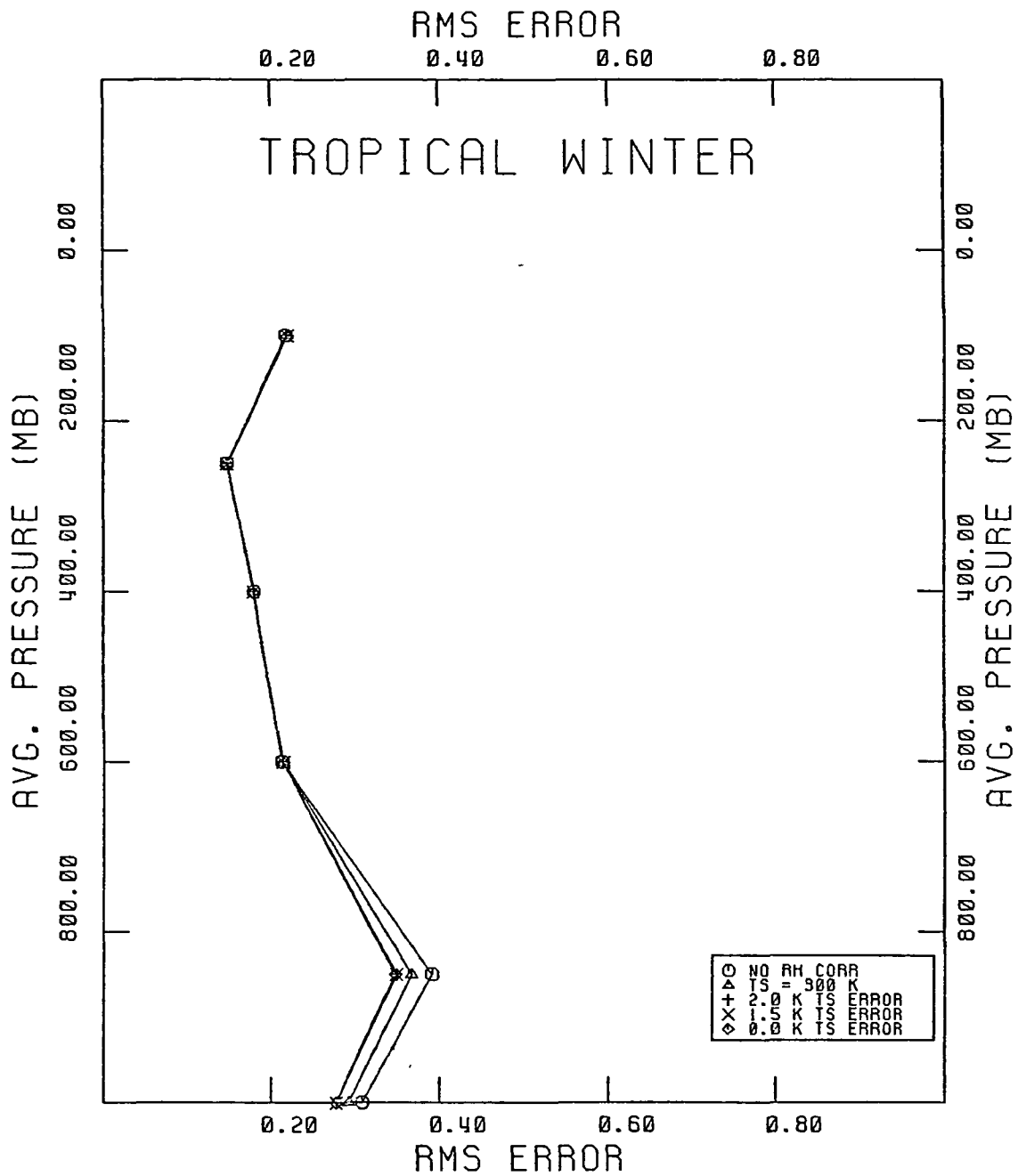
Figure 3-4. Effect of surface layer relative humidity adjustment for supersaturation on first guess RMS errors for tropical winter atmospheres.

does improve the surface layer results by a few percent even when a constant surface temperature is assumed. Using a simulated retrieved surface temperature value does better still. Notably, this improvement is relatively independent of the surface temperature retrieval accuracy. Using the 1.5 K surface temperature retrieval accuracy value, an almost 12% relative improvement can be realized in retrieving the surface layer water vapor.

Figure 3-5 illustrates the combined effect of relative humidity correction and uncertainty in the retrieved temperature profile on the RMS error of the layer water vapor retrieval. The first guess curve includes 1.5 K temperature profile error, but no relative humidity correction near the surface. The relative humidity correction adopted assumes a 1.5 K error in surface temperature retrieval. Consistent with the discussion in Section 3.5, the effect of temperature profile error reduction from 1.5 to 1.0 K is chiefly noted in the upper atmosphere.

3.7 Summary of First Guess Results

The first guess water vapor retrieval algorithm was applied to each of the five atmospheric sounding sample independent sets defined in Table 2-1. The format adopted as the standard algorithm for this purpose included the linear fit of column integrated values from the respective dependent set (§3.2), power law smoothing of the retrieved integrated profile (§3.3), an assumed temperature profile error of 1.5 K (§3.5), and the relative humidity correction of the surface layer values with an assumed surface temperature retrieval error of 1.5 K (§3.6). Results are given in Figure 3-6 (climatologies for comparison are shown in Figure 2-8) and can be understood largely on the basis of the scatter diagrams illustrated in Figure 2-13 upon which the first guesses are based. The high RMS errors for the upper levels of the midlatitude atmospheres (MS, MW) are probably in large part due to an extrapolation of the profiles above the values given by the 1700 cm^{-1} channel to tropical rather than the appropriate midlatitude values. The RMS error minimum for both the layers centered at 250 mb (for the tropical atmospheres sets) and at 400 mb for all of the sets is undoubtedly due to the influence of the 1650.1 and 1839.4 channels in providing accurate column amounts. For the two surface layers (centered at 600 and 850 mb, respectively), RMS error is related to the degree of scatter in the log integrated water/brightness temperature fit for the channels peaking in the lower atmosphere. The RMS
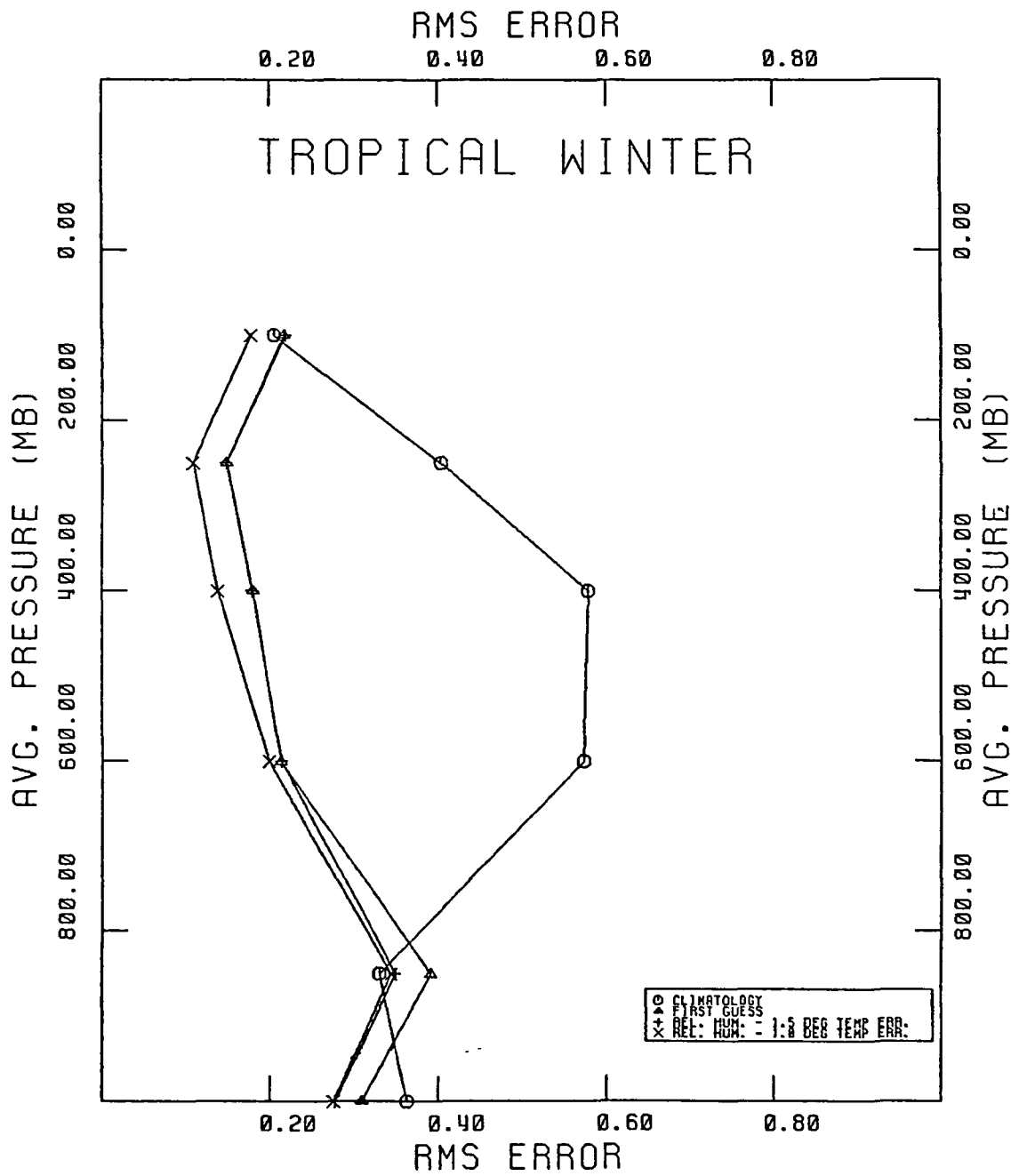
Figure 3-5. Combined effect of surface layer relative humidity adjustment
and simulated temperature profile error on first guess RMS
errors for tropical winter atmospheres.
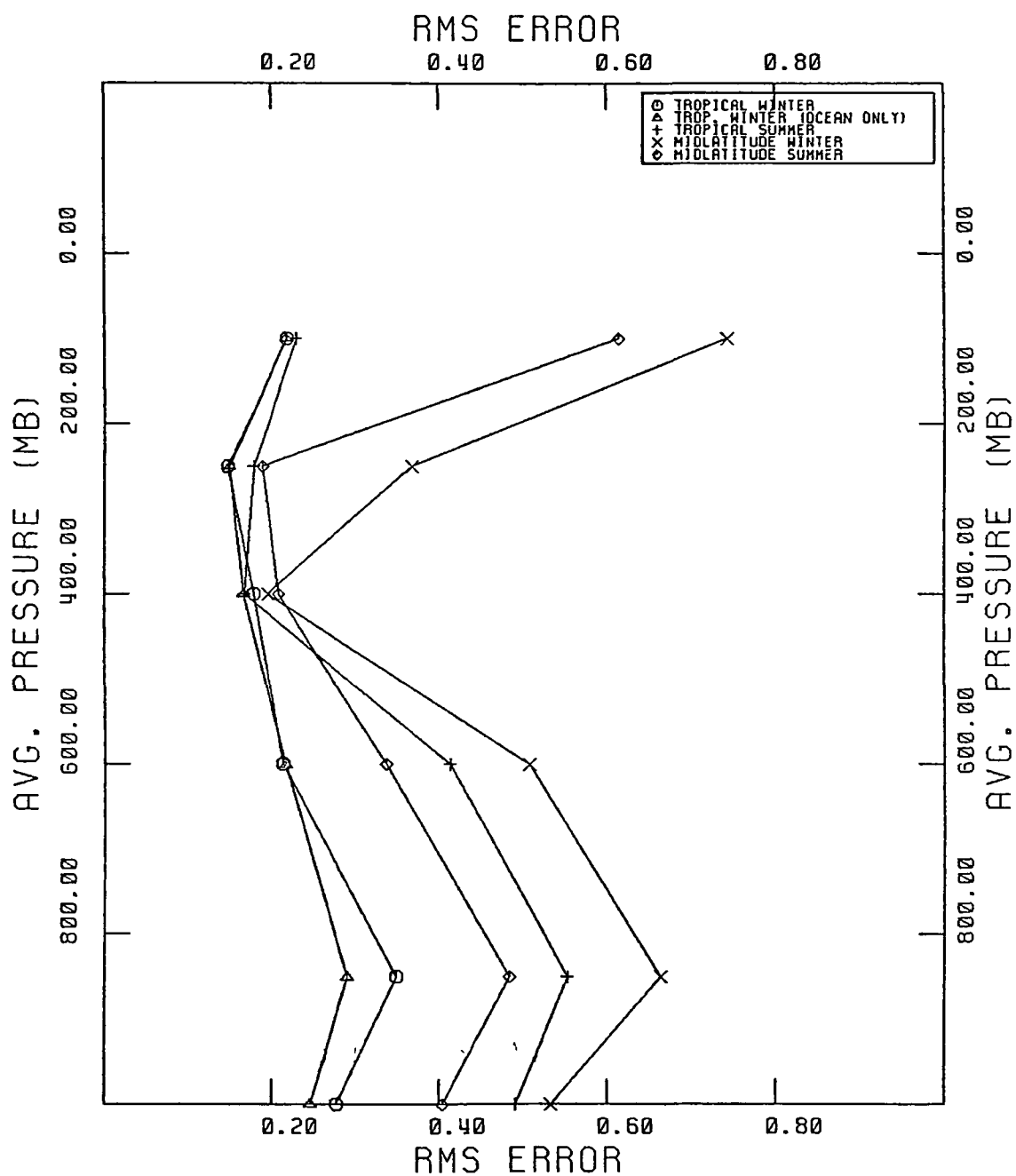
Figure 3-6. RMS errors of first guess layer water vapor values for tropical winter, tropical winter (ocean only), tropical summer, midlatitude winter, and midlatitude summer atmospheres.

error performance in the surface layer by atmospheric set is that given by the ability of the 1930.1 cm^{-1} channel to retrieve column integrated amount within the context of the first guess method, i.e. in order of increasing accuracy: midlatitude winter, tropical summer, midlatitude summer, and tropical winter. The specially processed tropical winter set using soundings over the ocean probably does best mostly because it has the least number of soundings with dry lower layers. In order to improve the first guess algorithm in the lower atmosphere, especially for the midlatiude soundings, it will be necessary to investigate more advantageous column retrieval approaches.

4. RELAXATION OF FIRST GUESS RETRIEVALS

4.1 Relaxation Algorithm

Although the first guess algorithm described in the previous section produces skillful retrievals throughout much of the atmosphere, it is desirable to take advantage of the sensitivity of the selected water vapor channel set to further reduce remaining errors. This is of particular value for the layers above 200 mb for which the first guess does not provide much improvement over climatology. In order to accomplish this objective, the first guess layer water vapor values were used to start an iterative retrieval process based on the relaxation method (Chahine, 1968, 1970). The particular algorithm adopted is summarized in Figure 4-1.

The relaxation algorithm was formulated to retrieve atmospheric water vapor profiles (i.e. layer column values as described in §3.3 above) from noisy simulated sensor brightness temperatures, $\hat{T}_b^i$, [or equivalently their radiances $R^i(\hat{T}_b^i)$] calculated from the independent set of soundings. The six AMTS channels (or alternatively, the four HIRS channels) used in the first guess algorithm were also used as input for the relaxation code. A retrieved temperature profile, $\hat{T}(p)$, and surface temperature, $\hat{T}_s$, were also assumed known, each with 1.5 K of retrieval error (2.0 K for HIRS). For each attempted retrieval, the relaxation process was started using the first guess integrated water vapor profile, $U_o(p)$, obtained using the methodology described in Section 3.2 above and the rapid algorithm (Susskind et al., 1982) to evaluate radiances for each channel, $R_o^i[U_o(p), \hat{T}(p), \hat{T}_s]$. The need for subsequent relaxations was based on examining the residuals for each channel given by:

$$\Delta_n^i = \frac{R_n^i - R^i(\hat{T}_b^i)}{R^i(\hat{T}_b^i)} \tag{4.1}$$

Two formats were used in this decision: (a) without constraints or (b) with constraints. In the former cases, a fixed number of relaxations (say three or ten) were employed, regardless of the residual values. For the latter cases, relaxation of a particular channel was terminated when either the residuals increased or when they were reduced below a predetermined noise threshold.

The following sections discuss the relationship used to relax water vapor values during the retrieval process, the effect of temperature profile errors
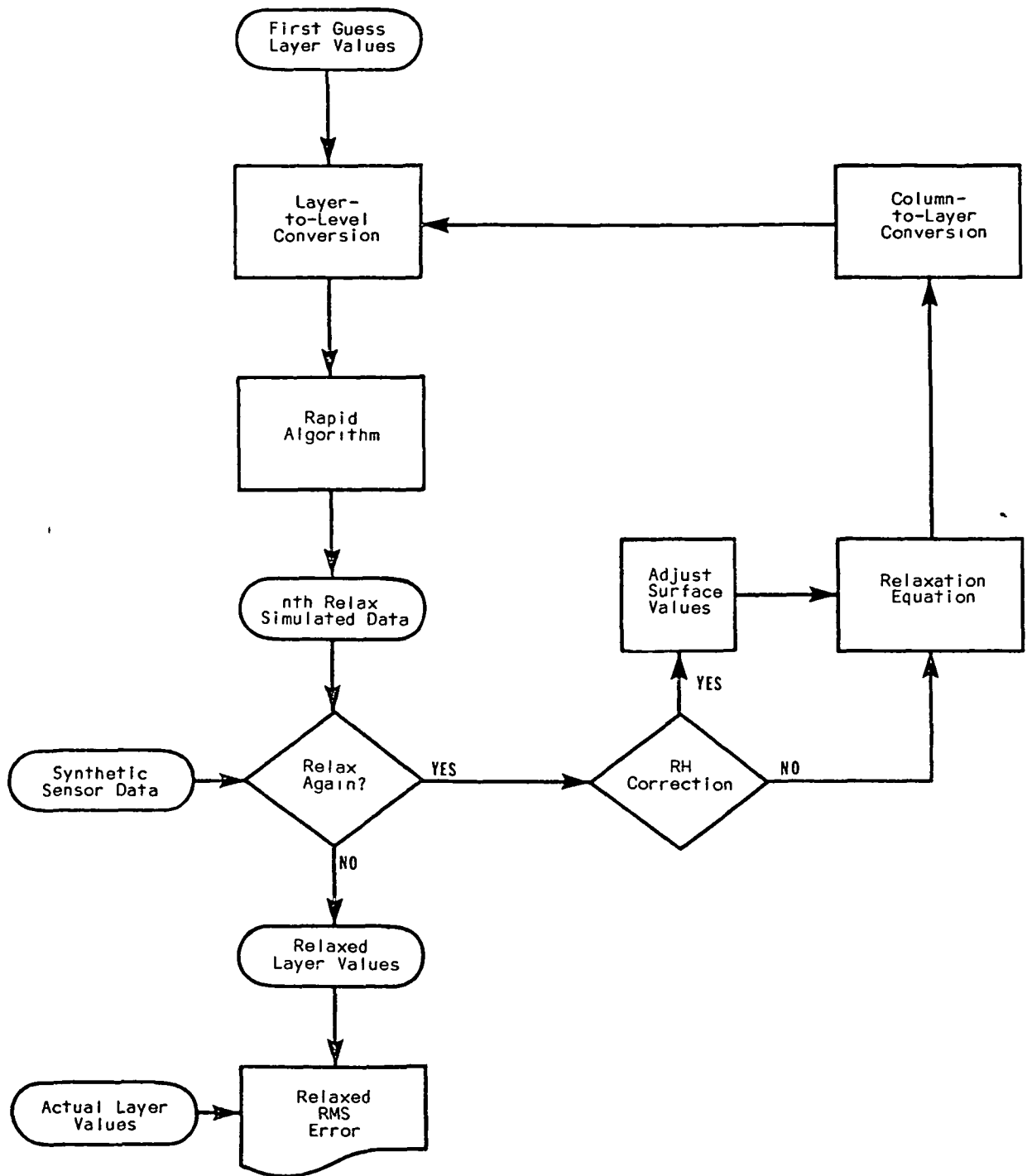
Figure 4-1. Schematic of the Relaxation Program

and the use of various constraints to terminate channel relaxation, and finally retrieval results for both AMTS and HIRS for the atmospheric sounding sets defined above.

4.2 The Relaxation Equation

The relaxation equation adopted for determining the water vapor column to pressure level $p(T = T_b^i)$ from the ith channel radiance was

$$\frac{R^i(\hat{T}_b{}^i)}{R_n^i} \approx \frac{\int \tau_{n+1}^i dB}{\int \tau_n^i dB} \approx \frac{\tau_{n+1}^i [P(\hat{T}_b^i)]}{\tau_n^i [P(\hat{T}_b{}^i)]} \tag{4.2}$$

where τ_n^i is the channel transmittance for the nth relaxation. It is partially based on the assumption of a random strong line relationship $(\tau_i \approx \exp(-a_i U^{1/2}))$ between transmittance and integrated water vapor, resulting in:

$$U_{n+1} = U_n (1 + \ln[R^i(\hat{T}_b^i)/R_n^i]/\ln \tau_n^i)^2. \tag{4.3}$$

4.3 Factors Influencing Relaxation Results

Although the volume of our relaxation tests has been limited in scope, five factors have been identified which apparently influence the accuracy of resultant water vapor retrievals. In approximate order of increasing importance as they influence retrieval accuracy these are: (1) temperature profile error, (2) number of iterations, (3) constraints used to terminate the relaxation process, (4) accuracy of first guess profile, and (5) water vapor channel set. To some extent, these factors are interrelated. For example, the number of iterations taken for a specific channel depends on the decision method used to terminate relaxing (if there is one). The water vapor channel sets (or alternatively, the sensor chosen) fixes the magnitude of temperature profile error and, as described in Section 3, also determines the accuracy of the first guess. It has also been noted previously that the first guess accuracy depends on the sample set of atmospheric soundings chosen for retrieval (i.e. midlatitude vs. tropical, etc.)

The effectiveness of the relaxation algorithm applied to the tropical winter set and AMTS instrument is illustrated in Figure 4-2. Here the ensemble RMS error was evaluated over the set of 100 independent TW soundings
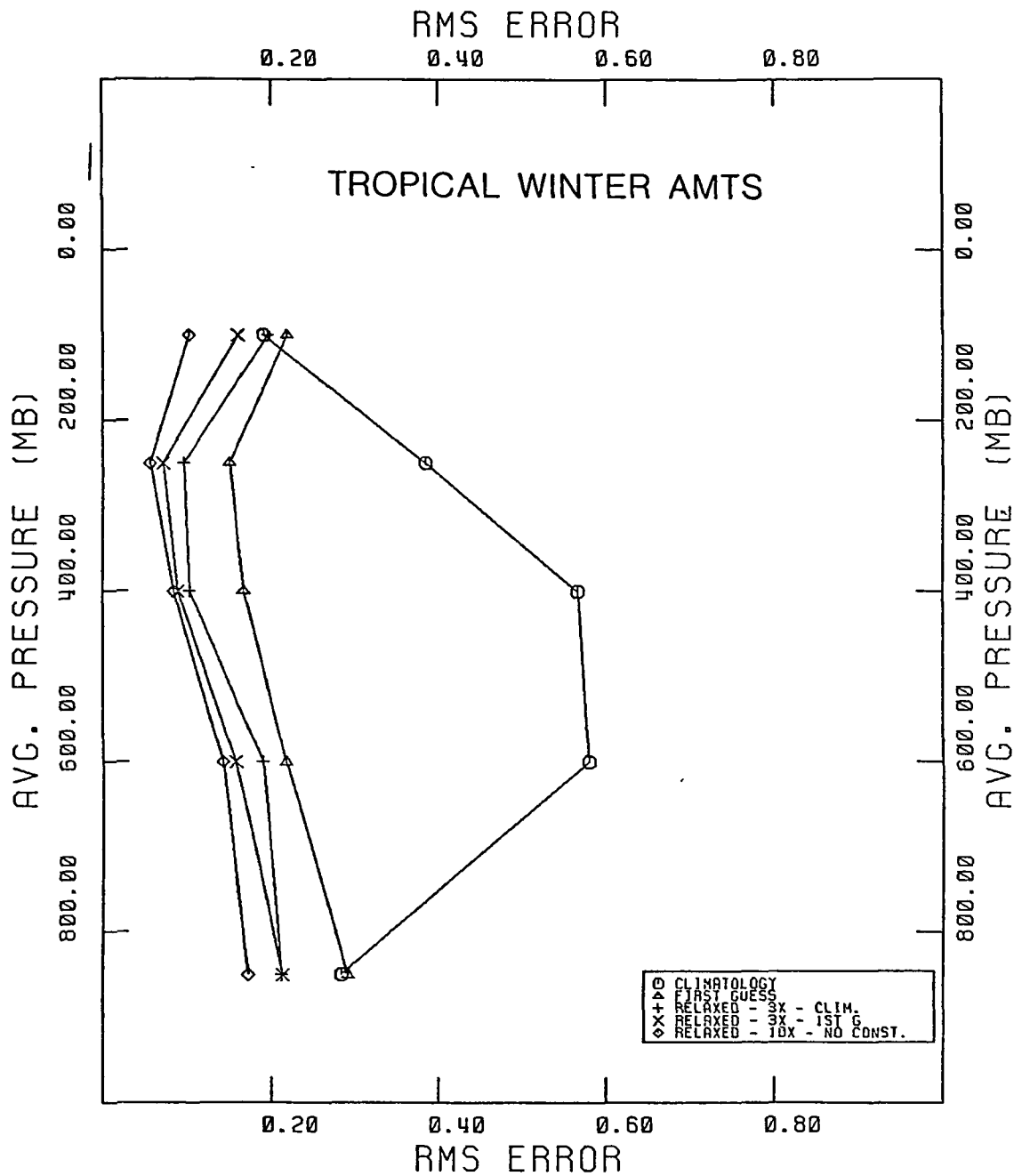
Figure 4-2. Comparison of RMS error in water vapor retrieval results for Tropical Winter (ocean only) atmospheres relaxed using climatology as a first guess (3 iterations), and the first guess results as a first guess (for both three and ten iterations).

for layer water vapor profiles relaxed using: (a) climatology (i.e., the mean profile from the dependent TW set) as first guess (relaxed three times with constraints), (b) the first guess as first guess, and (c) the first guess but relaxed ten times with no constraints. The assumed temperature profile error for AMTS was 1.5 K. Both the variability of the dependent sounding set (i.e. climatology) and the first guess retrieval are included for comparison. for this set of soundings, the relaxation method significantly improves the accuracy of water vapor retrievals obtained using the first guess algorithm alone. Notably, the relaxed results obtained using the first guess as the starting water vapor profile are somewhat better than those similarly obtained starting with climatology.

The best results overall are those relaxed ten times for each channel without terminating relaxation in any channel (i.e. no constraints). The figure of ten relaxations was chosen for convenience and does not represent the result of an optimized relaxation procedure. The degree of improvement noted for this case is uniform for each layer compared to the initial first guess results. This is not true for the cases performed with individual channel relaxations terminated when either the residuals increased or were determined to be below a numerical noise value (i.e. the constrained cases). These errors in the upper atmosphere increased with each relaxation.

The effect of these relaxation termination constraints is illustrated in Figure 4-3 for the AMTS instrument applied to the independent set of soundings for tropical summer. Three relaxations were done with and without individual channel relaxation termination. For comparison climatology, the corresponding first guess retrieval, and results for ten relaxations (without the contraints) are also included. Note that accuracy at upper levels is reduced by terminating the relaxation of individual channels. Examination of the residuals for these channels indicates that they relax very early in the process (i.e. within one or two iterations). Terminating relaxation of these channels in subsequent iterations, however, allows noise to build up (i.e. their residuals actually increase) decreasing their impact on the retrieval accuracy. The effect of such noise can also be seen in the ten times relaxation results for the level values centered at 600 mb. There an increase in the number of iterations from three to ten actually increases the RMS error slightly although there is improvement over much of the profile, especially for the layers nearest the surface. In general, applying the relaxation
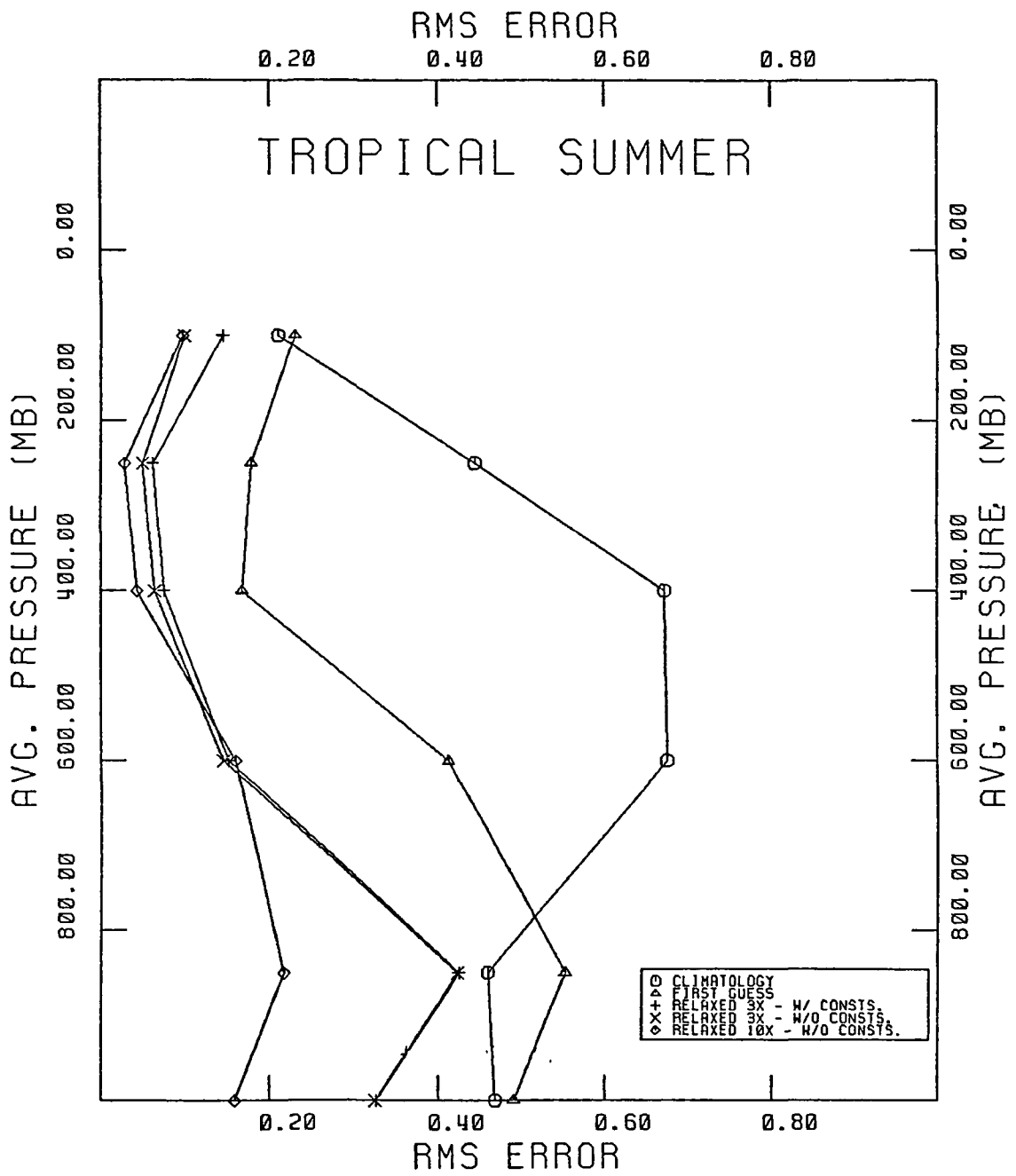
Figure 4-3. Effect of relaxation constraints on tropical summer water vapor retrievals using AMTS.

algorithm to AMTS, we have observed that the number of iterations required for residuals to stabilize at a minimum value is least for upper layers, greatest near the surface, and intermediate for the middle layers.

The effect of temperature profile retrieval accuracy on relaxation results is illustrated in Figure 4-4. Temperature profile error affects the water vapor retrieval relaxation process through the assignment of channel-dependent integrated column amounts to specific pressure levels based on comparison of brightness temperatures to the assumed temperature profile. Curves for three relaxations and temperature profile errors of 0.0 K, 1.5 K, and 2.5 K are illustrated. The first guess input profile illustrated for comparison was obtained assuming 1.5 K temperature profile error as is that for ten relaxations. As expected RMS error in layer water vapor retrieval increases with increasing error in the temperature profile at all levels. Notably, however, the spread in RMS water vapor error from 0.0 to 2.5 K temperature error is not great, i.e. temperature error does not greatly affect the relaxation results. Except for the level centered at 400 mb, for example, increasing the number of relaxations from three to ten improves the retrieval accuracy at all levels above that obtainable with no temperature profile error.

4.4 Comparison of AMTS and HIRS Instruments

First guess results for the AMTS and HIRS-2 instruments were used as initial guesses for the relaxation algorithms to provide the basis of an instrument comparison. Relaxation results were calculated for the tropical winter (ocean only), midlatitude summer, and midlatitude winter atmospheric sounding sets.

Figure 4-5 compares relaxations for HIRS-2 and AMTS using corresponding first guess inputs. For the same number of relaxations (term with no constraints), AMTS outperforms HIRS-2. Comparing the first guess and relaxed RMS error statistics for each instrument, the improvement due to relaxation of the first guess is quite nonuniform for HIRS. Accuracy in the upper layers is markedly improved while that near the surface responds little. As remarked earlier, it is much more uniform for AMTS. A possible explanation of this discrepancy is the applicability of the relaxation equation used at each iteration (cf. Section 4.2) to the specific spectral properties of each instrument's channels. It is likely that the assumptions used in deriving the
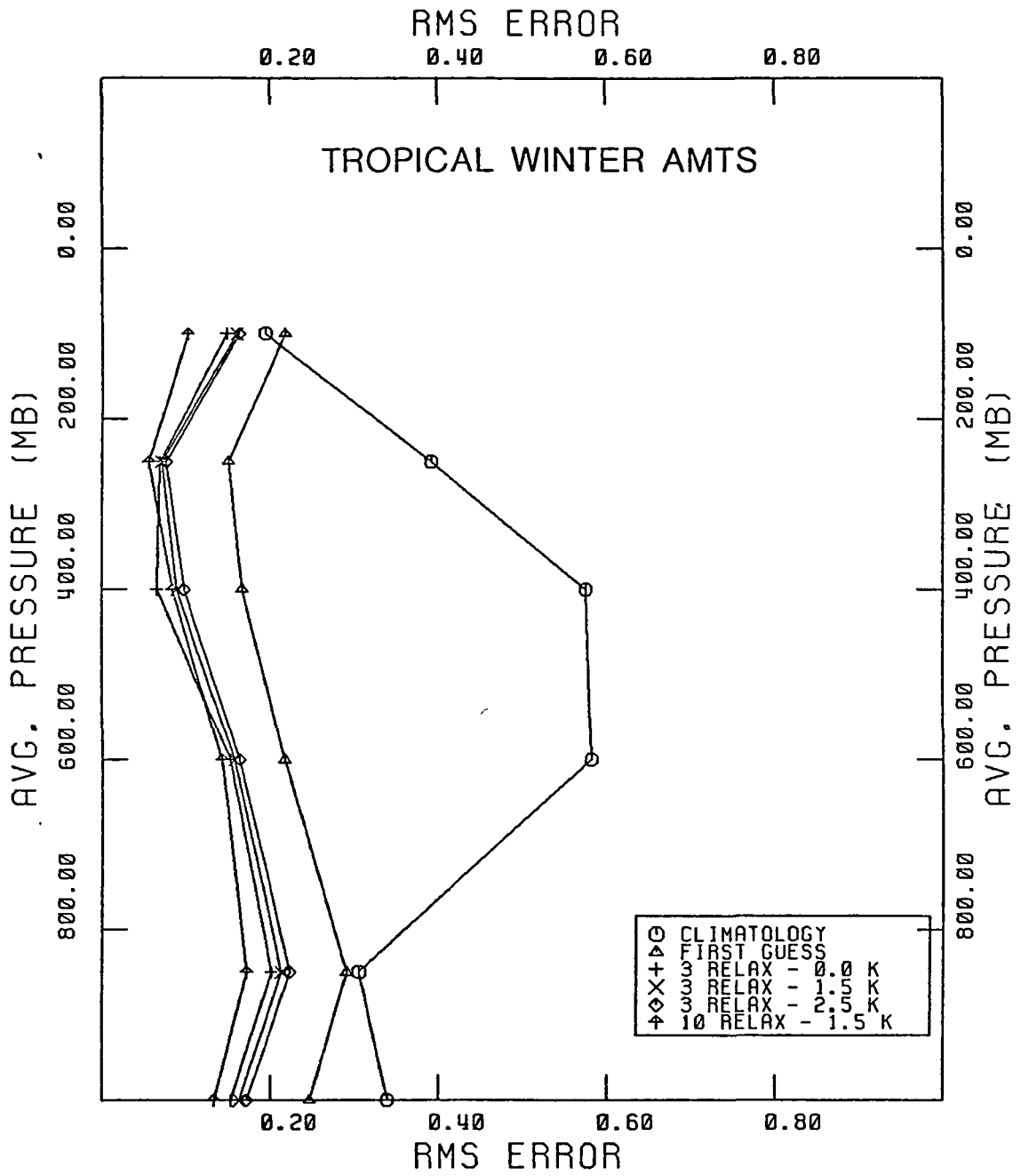
Figure 4-4. Effect of temperature profile error and number of relaxations on AMTS retrieval of layer water vapor values for tropical winter atmospheres (ocean only).

RMS ERROR

0.20   0.40   0.60   0.80

TROPICAL WINTER

AVG. PRESSURE (MB)

0.00
200.00
400.00
600.00
800.00

AVG. PRESSURE (MB)

0.00
200.00
400.00,
600.00
800.00

⊙ CLIMATOLOGY
△ HIRS - FIRST GUESS
+ AMTS - FIRST GUESS
✕ HIRS - RELAXED - 10X
◇ AMTS - RELAXED - 10X

0.20   0.40   0.60   0.80
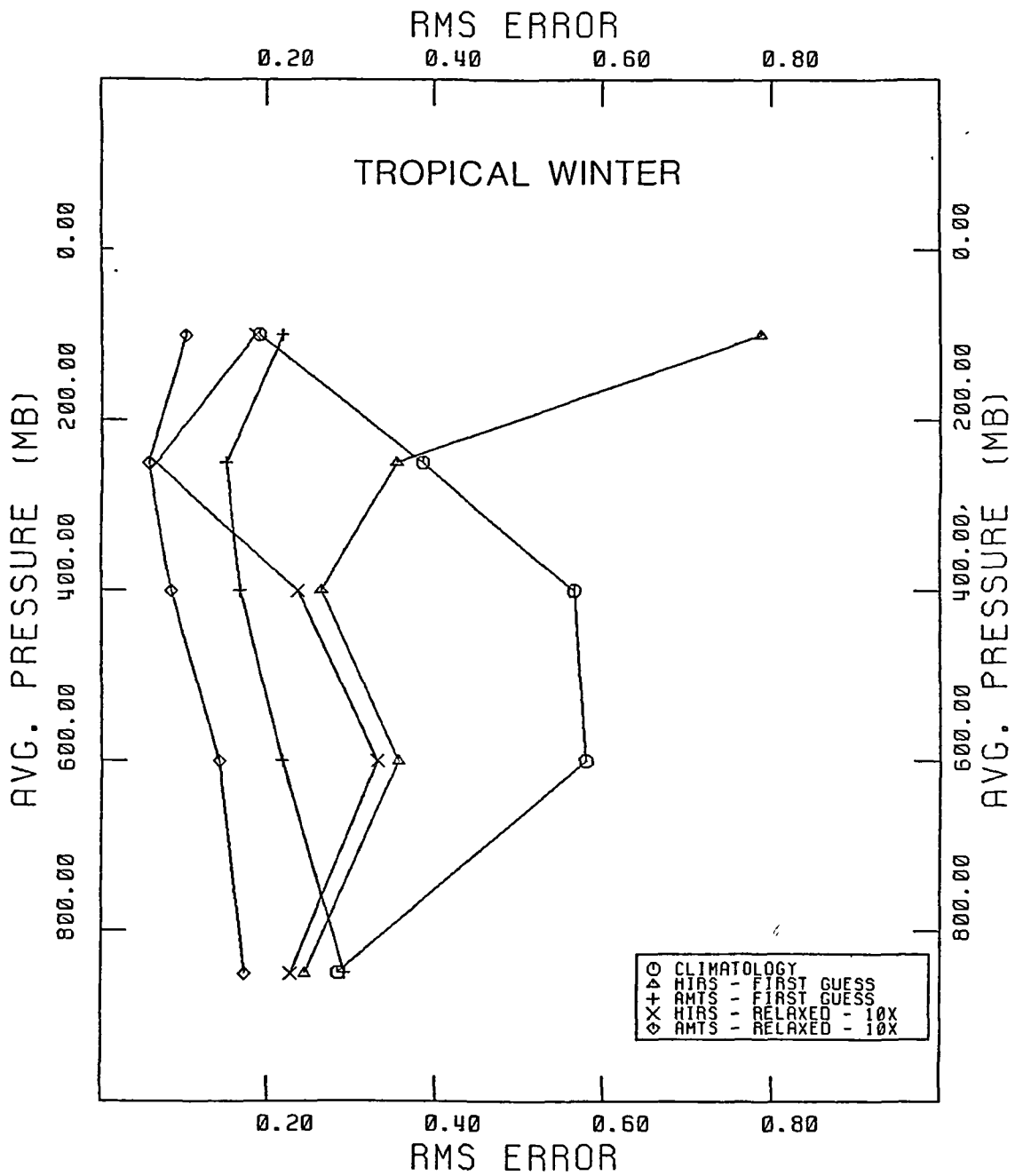
RMS ERROR

Figure 4-5.   Comparison of AMTS and HIRS first guess and relaxed RMS
errors in retrieved water vapor for tropical winter
(ocean only) atmospheres.

relaxation criteria (i.e., random strong lines) is most applicable to the most opaque HIRS-2 channels, i.e. those affecting the retrieval of upper layers. Additionally, most of the information available from the HIRS-2 channels affecting the lower atmosphere, is probably already in the first guess.

Analogous results for the midlatitude summer sounding set is shown in Figure 4-6. In this case the better HIRS first guess in the layer near the surface gives it an advantage in the subsequent relaxation processes. Throughout much of the rest of the atmosphere, however, the converse is true, with the relaxed AMTS results providing more accurate retrievals. As as noted in the discussion of Figure 4-5, the upper layer HIRS results relax considerably over those of the first guess while those near the surface change little.

Finally, Figure 4-7 compares HIRS and AMTS for the midlatitude winter sounding set. As noted previously, first guesses for this set are not particularly good due to the poor column integrated water/brightness temperature relationships derived from the dependent set. Like the MS set results above (with the exception of the layer centered at 250 mb), the AMTS first guess results are slightly better in the upper layers, while HIRS better predicts the surface layer values. Upon relaxing a like number of times (in this case six with constraints), RMS errors increase in the lower atmosphere for the HIRS instrument while decreasing for the AMTS.

RMS ERROR

0.20   0.40   0.60   0.80

MIDLATITUDE SUMMER

AVG. PRESSURE (MB)

0.00 200.00 400.00 600.00 800.00

AVG. PRESSURE (MB)

0.00 200.00 400.00 600.00 800.00

⊙ CLIMATOLOGY
△ HIRS - FIRST GUESS
+ AMTS - FIRST GUESS
✕ HIRS - RELAXED - 3X
◇ AMTS - RELAXED - 3X

0.20   0.40   0.60   0.80
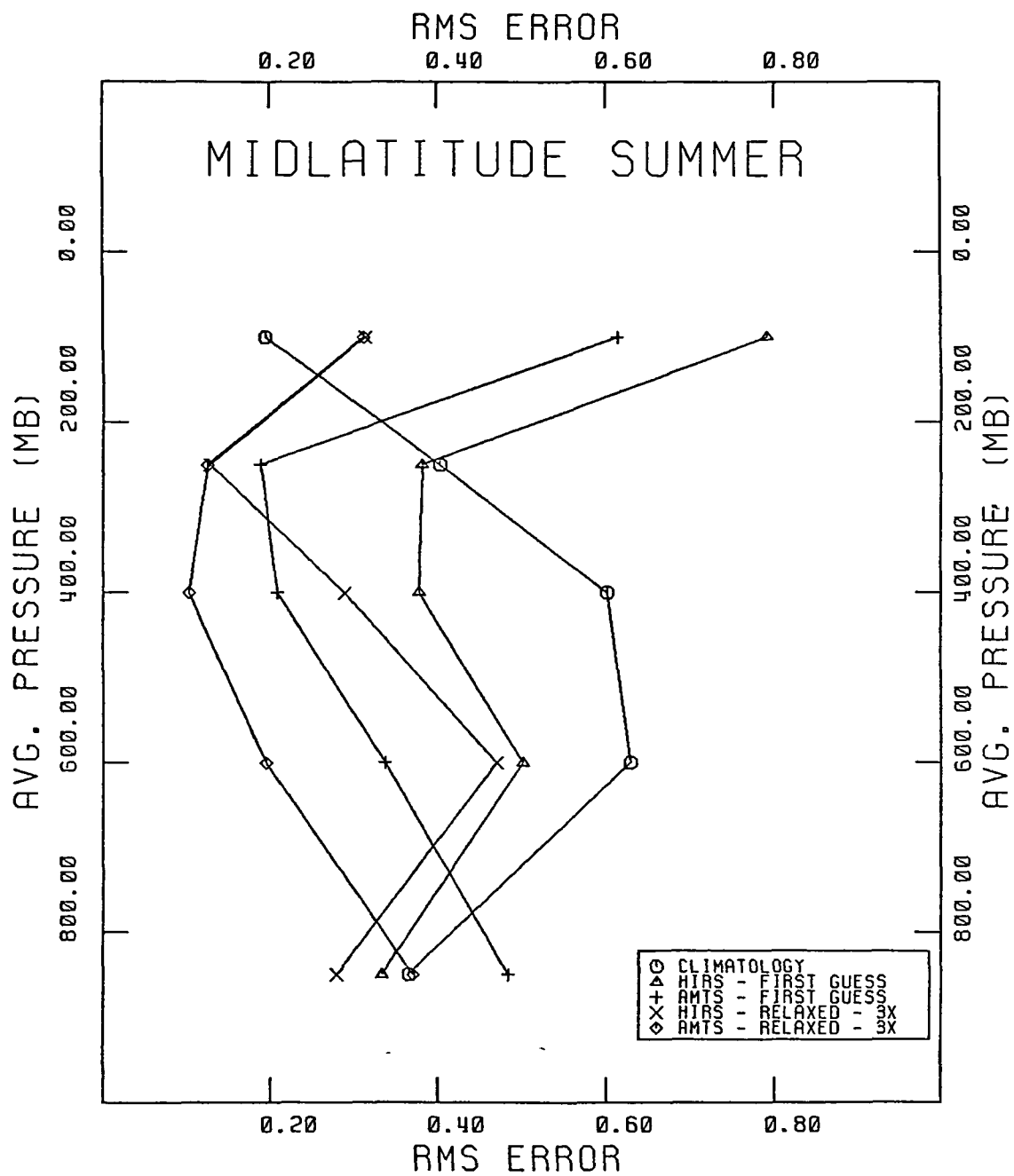
RMS ERROR

Figure 4-6. Comparison of AMTS and HIRS first guess and relaxed RMS
errors in retrieved water vapor or midlatitude summer
atmospheres.

-56-
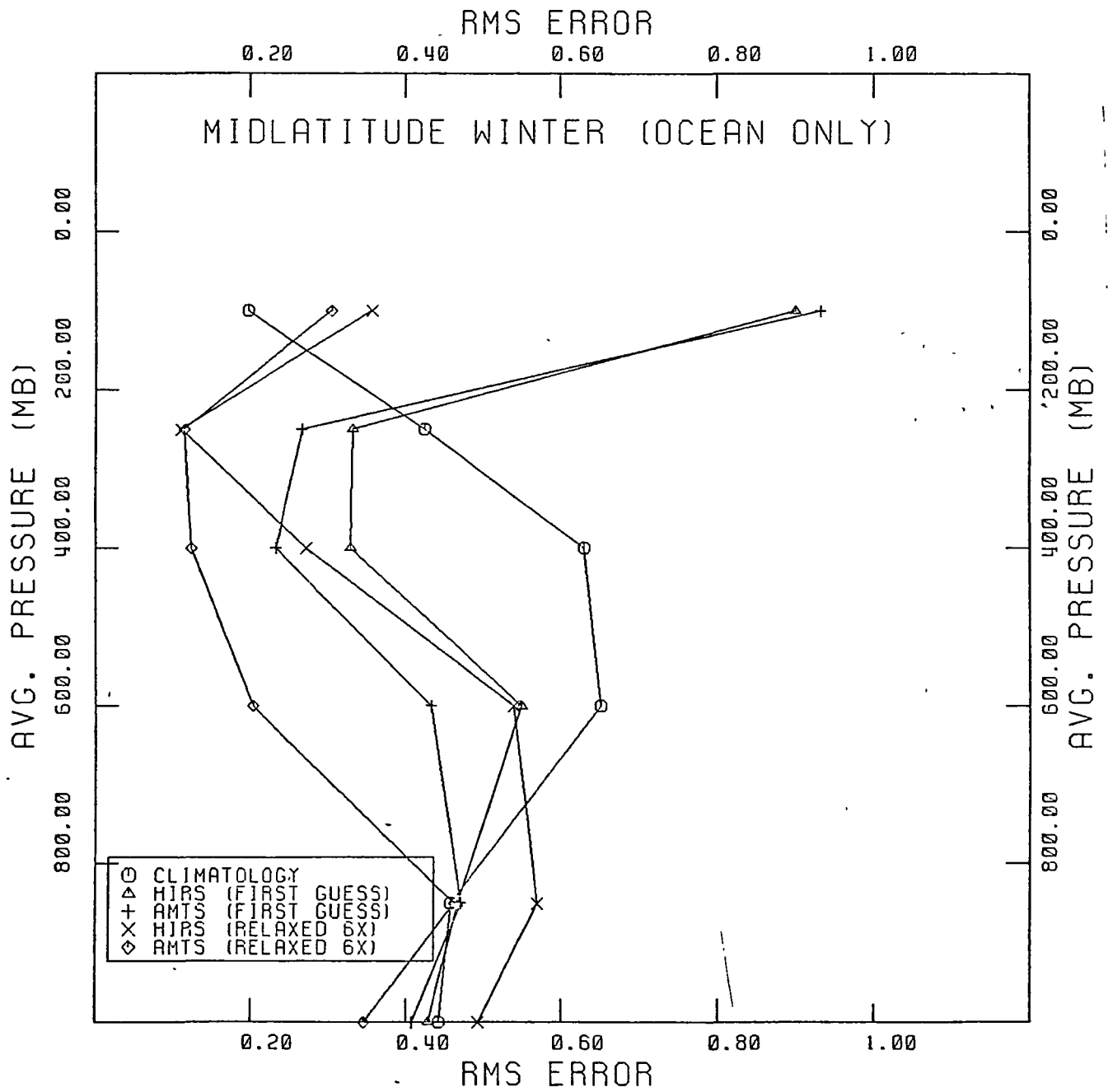
Figure 4-7. Comparison of AMTS and HIRS first guess and relaxed RMS
retrieval errors for midlatitude winter atmospheres
compared to climatology.

5. STATISTICAL RETRIEVAL OF WATER VAPOR

5.1 Background and Methodology

As the last stage in this abbreviated effort, the first guess and relaxed physical retrieval simulations described above were compared with statistical retrieval simulations, described in this section. The statistical moisture profile retrievals were obtained based on inverting the independent samples of simulated sensor brightness temperatures calculated using the simulation code described in the previous sections and implementing an inversion technique based on an approach to obtaining geophysical parameters from radiometric data discussed by Rodgers (1966), Staelin (1967), Gaut (1967), Waters and Staelin (1968) and Gaut (1968). It is similar to the procedure outlined in Westwater and Strand (1965). The method is reviewed by Rodgers (1976). The essential element of the scheme is to choose, in a statistical sense, the most probable combination of atmospheric and surface properties which produces the set of measured radiometric data values. It is a general statistical regression technique which minimizes the mean square error between the estimated and observed values of the parameter of interest. This method is also similar to that used operationally for obtaining microwave temperature profiles from the SSM/T (Rigone and Stogryn, 1977; Grody et al., 1984) and proposed as the basis of an approach to millimeter moisture retrieval by Rosenkranz et al. (1982). As applied in our retrievals, layer water vapor abundances obtained from the dependent sample set of radiosondes were regressed directly against the respective brightness temperatures obtained by stimulation. Retrievals were accomplished by using these regression statistics and simulated sensor brightness temperatures for the independent sample to obtain analogous layer abundances. The parameter retrieved was the absolute abundance of water vapor (molecules cm^{-2}) in six layers corresponding to 0-200, 200-300, 300-500, 500-700, 700-850 mb, and 850-1000 mb, respectively.

More precisely, the technique consisted of calculating and using the eigenvectors of covariance matrix of the data set (here brightness temperatures) with itself and of the parameter set (here layer integrated water vapor) with itself (see Smith and Woolf, 1976). An individual retrieval of layer integrated water vapor in the six layers from n channel brightness temperatures was obtained from:

$$\hat{u} = D\hat{t} \qquad\qquad (5.1)$$

with

$$D = (UT^t)(T*\Lambda*^{-1}\hat{T}*^t) \qquad\qquad (5.2)$$

where

u   is a vector giving an estimate of the profile of integrated water vapor in each of six layers

t   is a vector whose components are n brightness temperatures

U_{rs} water vapor at six levels for s atmospheric samples (r=6)

T_{ns} brightness temperatures for n channels for s samples

T*   selected eigenvectors of TT^t

Λ*   diagonal matrix whose elements are corresponding eigenvalues

The eigenvectors having relatively small eigenvalues (compared with the largest eigenvalue) can be discarded since they represent noise. In the algorithm employed, only eigenvectors of the covariance matrix of the data set with itself have the potential to be discarded. The advantage of the method is that by truncating the sequence of eigenvalues, one reduces the condition number of the matrix, and therefore also the sensitivity to noise. (As it turns out, none of the eigenvalues of the covariance matrix of the parameter set with itself are small enough to be discarded using a criteria of 10^{-6}. Thus all of them need to be retained.) In this method, if none of the eigenvectors are discarded, the problem reduces to that of solving the least squares fit problem, i.e.

$$D = UT^t(TT^t)^{-1} \qquad\qquad (5.3)$$

A quantitative measure of retrieval accuracy was obtained by comparing inferred layer water vapor abundances to those in the actual profiles (the error) and evaluating the fractional root mean square (RMS) error over the ensemble of retrievals. The RMS error for each layer k evaluated over the set of N = 100 independent soundings was again defined as:

of N = 100 independent soundings was again defined as:

$$RMS(k) = \frac{1}{\bar{u}(k)} \left\{ N^{-1} \sum_{j=1}^{N} \left[\hat{u}(k,j) - u(k,j) \right]^2 \right\}^{1/2} \qquad (5.4)$$

where $\hat{u}(k,j)$ and $u(k,j)$ are, respectively, the retrieved and actual water vapor amounts for the kth layer and j^{th} sounding and $\bar{u}(k)$ is the layer mean value. For comparison, the same statistic was evaluated assuming the mean of the ensemble as the best estimate climatological retrieval for each sounding, i.e. by replacing $\hat{u}$ by $\bar{u}$ itself. The ratio of the fractional RMS error of the retrievals to that of climatology provides a direct measure of retrieval effectiveness. The former quantity should always be less than the latter. (When this is not true the retrieval process itself has usually added too much noise.) The fraction of unexplained variance (FUV), an often used statistic, is the square of this ratio. When the two quantities are equal, the FUV is unity and no information has been gained from the retrieval process. When the FUV is zero, the retrieval is perfect.

5.2 Comparison of Retrieval Simulation Results

Figure 5-1 compares the RMS fractional errors for simulated statistical retrievals of tropical winter ocean (TWO) soundings from measurements by AMTS, HIRS, AMSU-B, and SSMT/2 instruments. It is seen that, at pressures greater than 750 mb, errors are nearly equal for all four instruments and less than those resulting from physical retrievals, as shown in Figure 4-5. At pressures less than 750 mb, the infrared retrievals are more accurate than the millimeter wave retrievals but become generally less accurate than the physical retrievals, at least in the case of AMTS. The almost identical error profiles for AMTS and HIRS statistical retrievals are in marked contrast to the systematic superiority of physical retrievals for AMTS relative to those for HIRS for tropical simulations. Similar results were found in tropical and midlatitude summer simulations.

RMS errors for AMTS and HIRS midlatitude winter statistical retrieval simulations are shown in Figure 5-2. Again, the error profiles are almost identical, AMTS being only marginally better. In this case, however, the statistical retrievals are better than the physical retrievals at all levels, as can be seen by comparing Figure 5-2 with Figure 4-7.

Figure 5-2. Same as 5-1 for midlatitude winter statistical retrievals for HIRS, AMTS, and climatology.

Figure 5-1. RMS errors for tropical winter ocean statistical retrievals from simulated measurements by HIRS, AMTS, AMSU-B, and SSMT/2, compared with climatology.

One implication of the above comparisons is that water vapor retrievals from AMTS measurements should be generally equal to or better than from HIRS or AMSU, at least for clear conditions. Supplementary microwave measurements would be desirable for overcast conditions, but our studies have found that the presence of clouds seriously degrades retrievals from measurements near 183 GHz, and requires extra channels to minimize cloud effects (Isaacs et al., 1985).

Another implication is that best results can be obtained by physical retrieval methods in the tropical and/or summer middle troposphere. Statistical retrievals seem to be generally more useful in the lower troposphere, and at all levels in middle (and presumably high) latitudes. It is still possible, however, that improved physical retrievals would result from the use of channels other than those used in this study. Some support for this possibility comes from the following examination of the separate contributions of the temperature and water vapor channels to the statistical retrievals.

5.3 Contributions of Temperature and Water Vapor Channels

The results reported for statistical retrievals from AMTS and HIRS in Figures 5-1 and 5-2 were obtained with the use of all the temperature channels, as well as the water vapor channels, in contrast to the physical retrievals reported earlier, for which only the water vapor channels were used, with the temperature assumed known within an RMS standard error. This approximates the way in which the physical and statistical retrievals would be done in practice, except that the temperature retrievals would be done first for a physical inversion, then water retrieval, then iteration.

Statistical inversion does not use a priori information except in the sense that it is included in the regression coefficients. Some insight into the information content of individual channels or sets of channels can be gained by examining the effect on RMS fractional errors of eliminating them in the statistical retrievals. This is illustrated for AMTS and HIRS tropical winter ocean statistical retrievals in Figure 5-3. The curves are, from left to right, for retrievals with the combined set of temperature and moisture channels as in Figure 5-1, for the temperature channels only, for the moisture channels only, and for climatology. Qualitatively similar results are shown in Figures 5-4 and 5-5, respectively, for summer and winter midlatitude retrievals. The temperature channels, labelled T and T_G, and moisture channels, labelled WV, are listed in Table 5, and consecutively numbered.
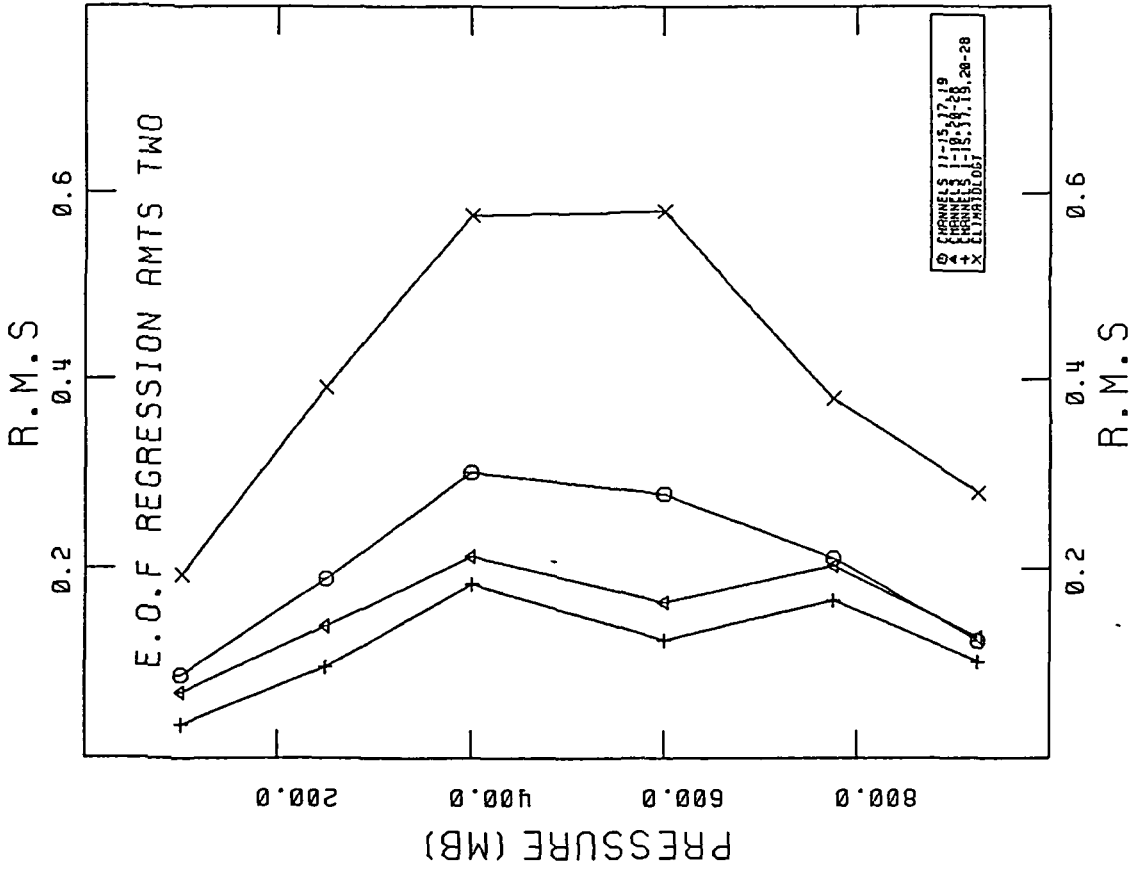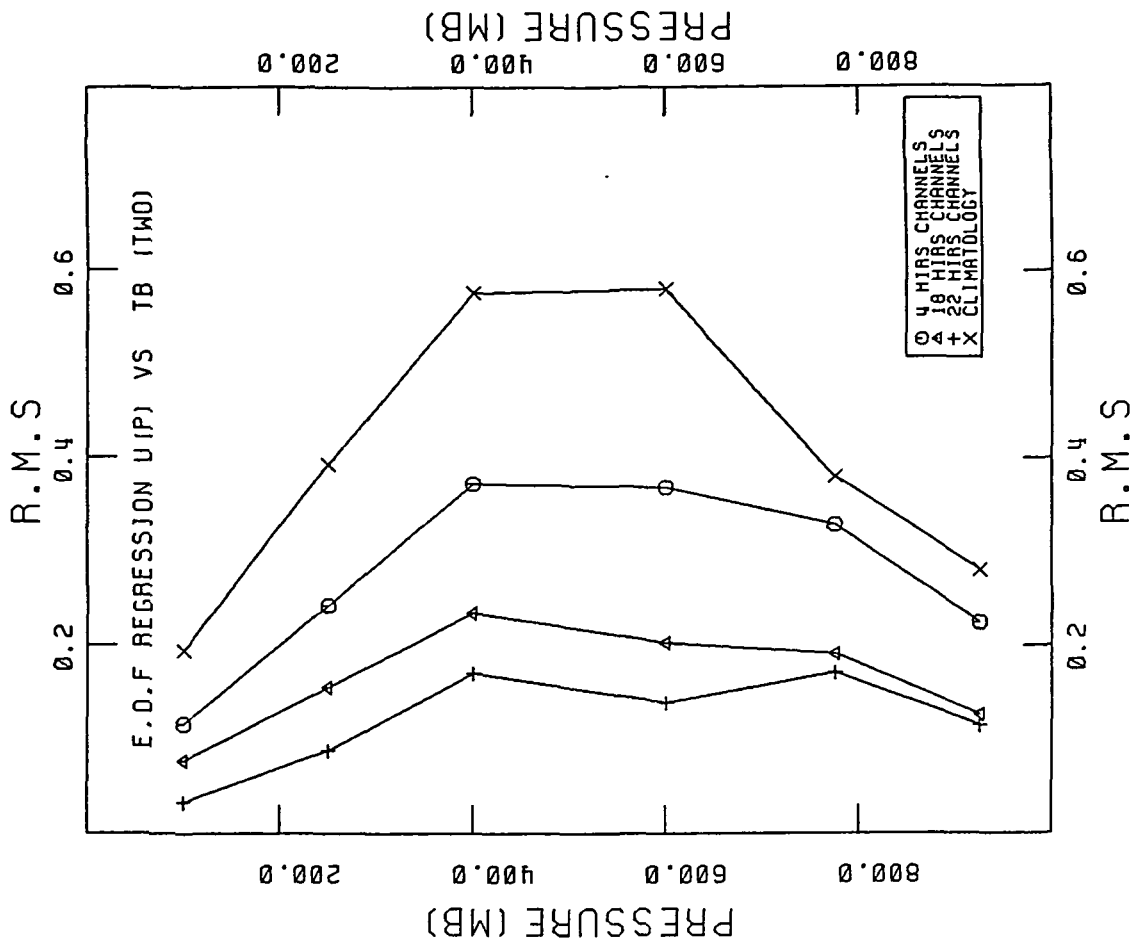
Figure 5-3. RMS errors for tropical winter ocean AMTS and HIRS statistical retrievals for combined temperature and moisture channels, for temperature channels only, for moisture channels only, and for climatology.
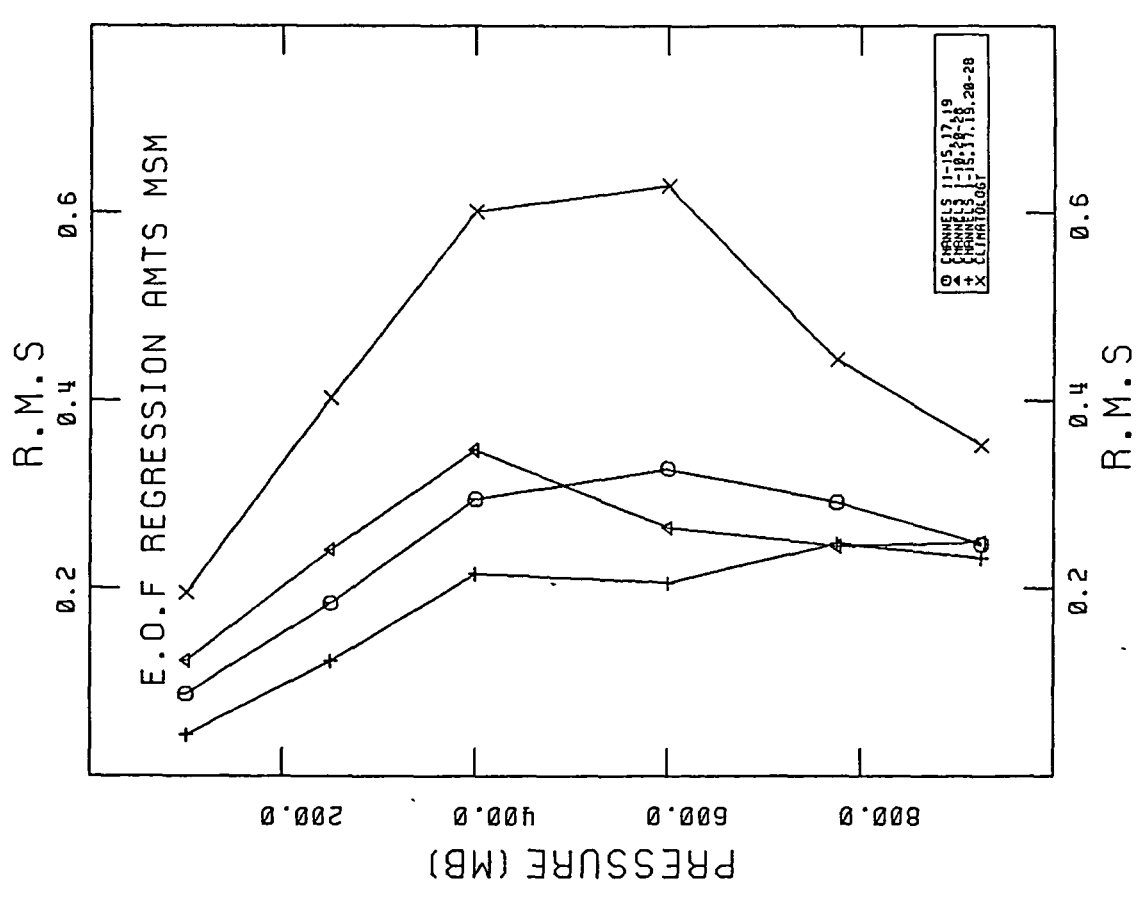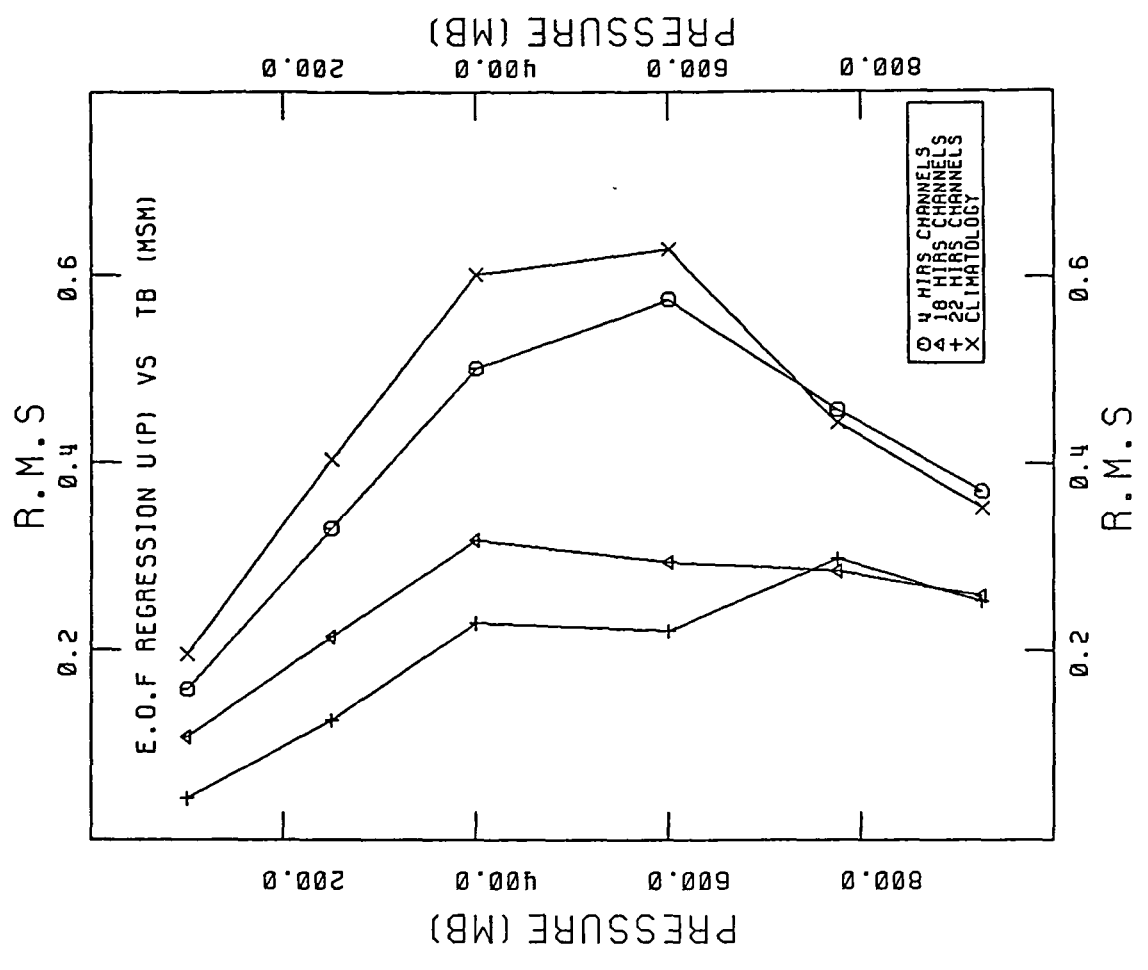
Figure 5-4. Same as 5-3, for midlatitude summer (MSM).
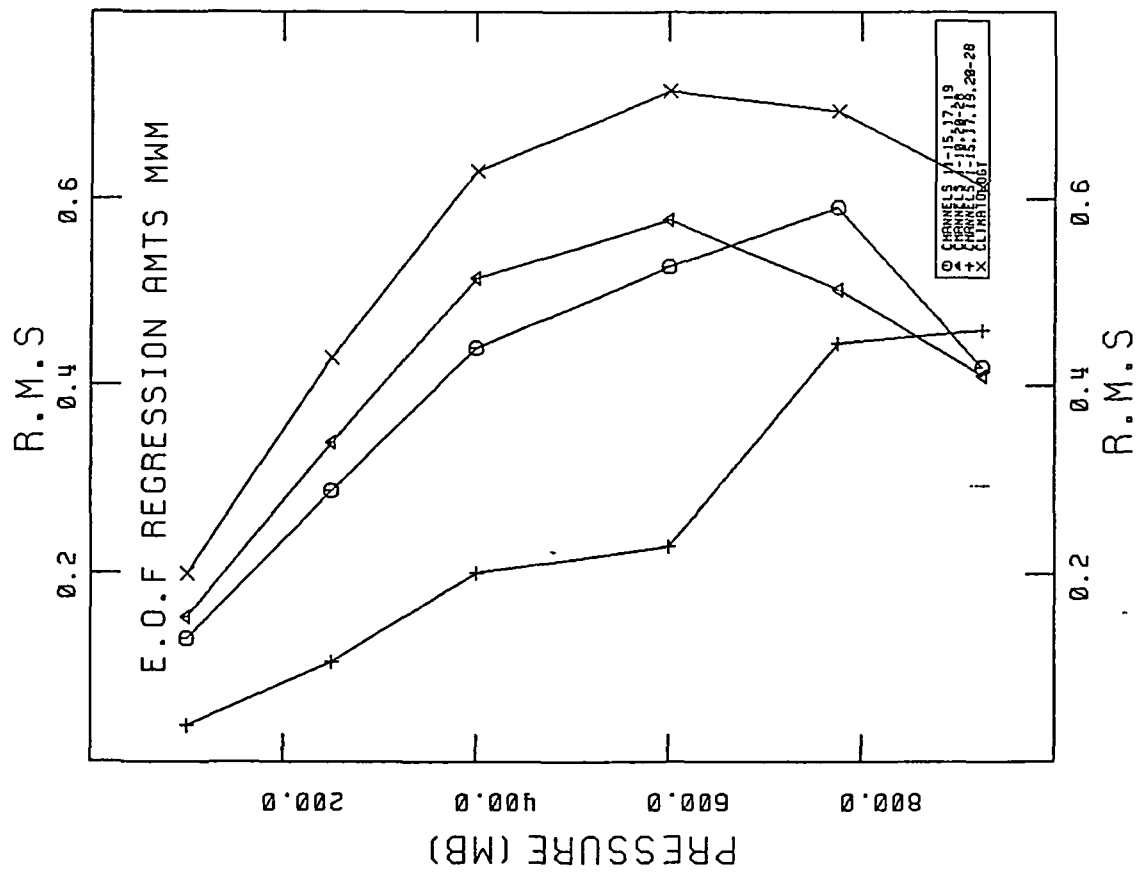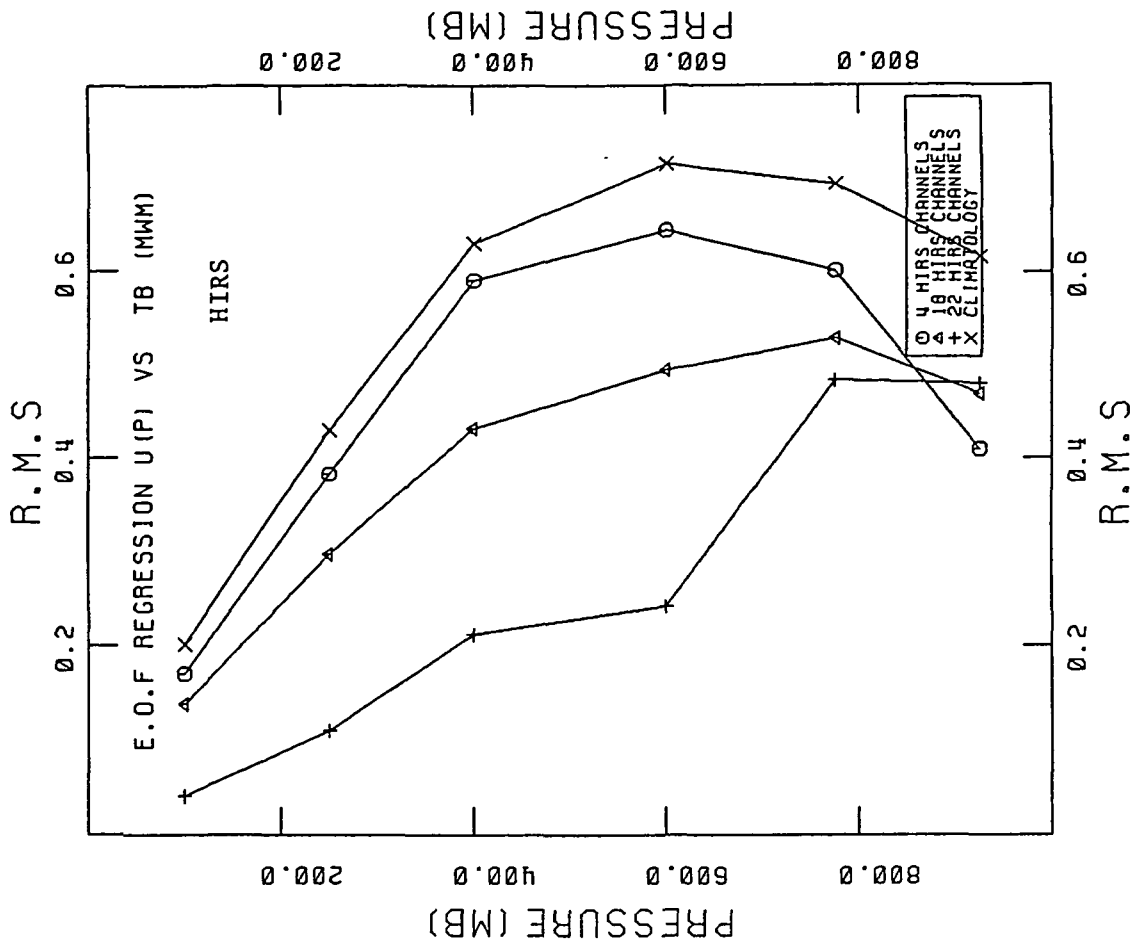
Figure 5-5. Same as 5-3, for midlatitude winter (MWM).

Table 5

AMTS and HIRS/MSU Temperature and Water Vapor Channels, and Water Vapor
Contribution to Temperature Channel Brightness Temperatures

No. (I)	AMTS ν cm^{-1}	AMTS Function	$\Delta T_B^i(C)$ TWO	$\Delta T_B^i(C)$ MWM	HIRS/MSU ν cm^{-1}	HIRS/MSU Function	$\Delta T_B^i(C)$ TWO
1	607.0	T	3.9	0.9	668.4	T	
2	623.2	T	3.7	1.2	679.2	T	
3	627.8	T	0.3	0.1	691.1	T	
4	634.3	T			703.6	T	0.4
5	646.6	T			716.0	T	1.1
6	654.4	T			732.4	T	2.7
7	665.6	T			748.3	T	4.6
8	666.8	T			897.7	WV	
9	668.2	T			1027.9	T_G, O_3	2.0
10	669.4	T			1217.1	WV	
11	875.0	WV			1363.7	WV	
12	1231.6	WV			1484.4	WV	
13	1650.1	WV					
14	1700.3	WV			2190.4	T	1.0
15	1839.4	WV			2212.7	T	0.6
16					2240.1	T	0.3
17	1850.9	WV			2276.3	T	
18					2511.9	T	0.2
19	1930.1	WV			2671.2	T	2.6
20	2384.0	T					
21	2386.1	T			50.3 GHz	T_G	-16.0
22	2388.2	T			53.7 GHz	T	-0.3
23	2390.2	T			55.0 GHz	T	
24	2392.4	T			58.0 GHz	T	
25	2394.5	T					
26	2424.0	T_G					
27	2505.0	T_G					
28	2686.1	T_G	0.4	0.1			

The AMTS moisture channel results are distinctly superior to those from HIRS, supporting the previous conclusion that the similar results from the physical retrievals are probably due to more moisture information in the AMTS channels. It is interesting that the statistical retrievals are considerably improved when the temperature channels are included, and particularly striking that use of the temperature channels alone give better results than use of the moisture channels alone. Part of the explanation, of course, is that the radiances in the moisture channels are functions of both the temperature and moisture distributions, and that there are more temperature channels than moisture channels. The question remains, however, as to whether the water vapor information in the temperature channels is mostly due to the well-known correlation between moisture and temperature in the atmosphere or to water absorption/emission in the temperature channels.

Two pieces of evidence supporting the latter cause are a much smaller improvement of statistical microwave retrievals by inclusion of the less moisture-sensitive temperature channels, and a marked deterioration of the retrieval when the most moisture-sensitive AMTS channels (channels 1 and 2, see Table 5) are removed. The moisture sensitivity is shown in Table 5 by the columns labelled $\Delta T_B^i(C)$, representing the increase in brightness temperature when the specific humidity is decreased by 99 percent at all levels. The effect of this temperature channel moisture sensitivity is shown in Figure 5-6 for TWO and MWM AMTS retrievals. The curves are, from left to right respectively, retrievals from all 19 temperature channels, a pair of almost identical retrievals with channels 1 and 2 missing, and with 1, 2, 3, and 28 missing, and finally climatology.

Evidently, the CO_2 absorption is helping to provide sharper effective water vapor weighting functions, even in the lower layers. The possibility of using these channels to improve physical moisture retrievals, therefore, seems well worth investigating. The possibility of finding even better new moisture channels in the 15 μ CO_2 band seems even more promising, since the temperature channels were deliberately chosen to minimize rather than maximize the effect of water vapor.
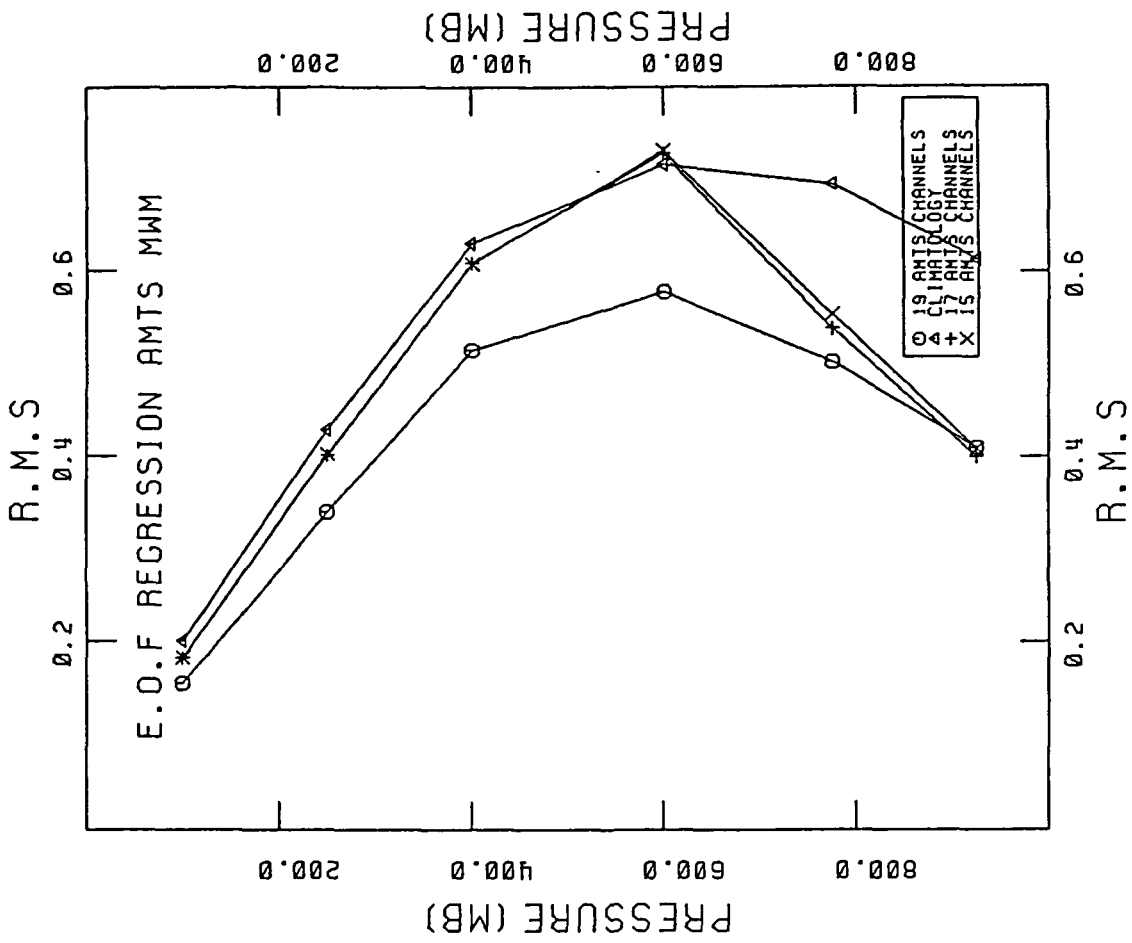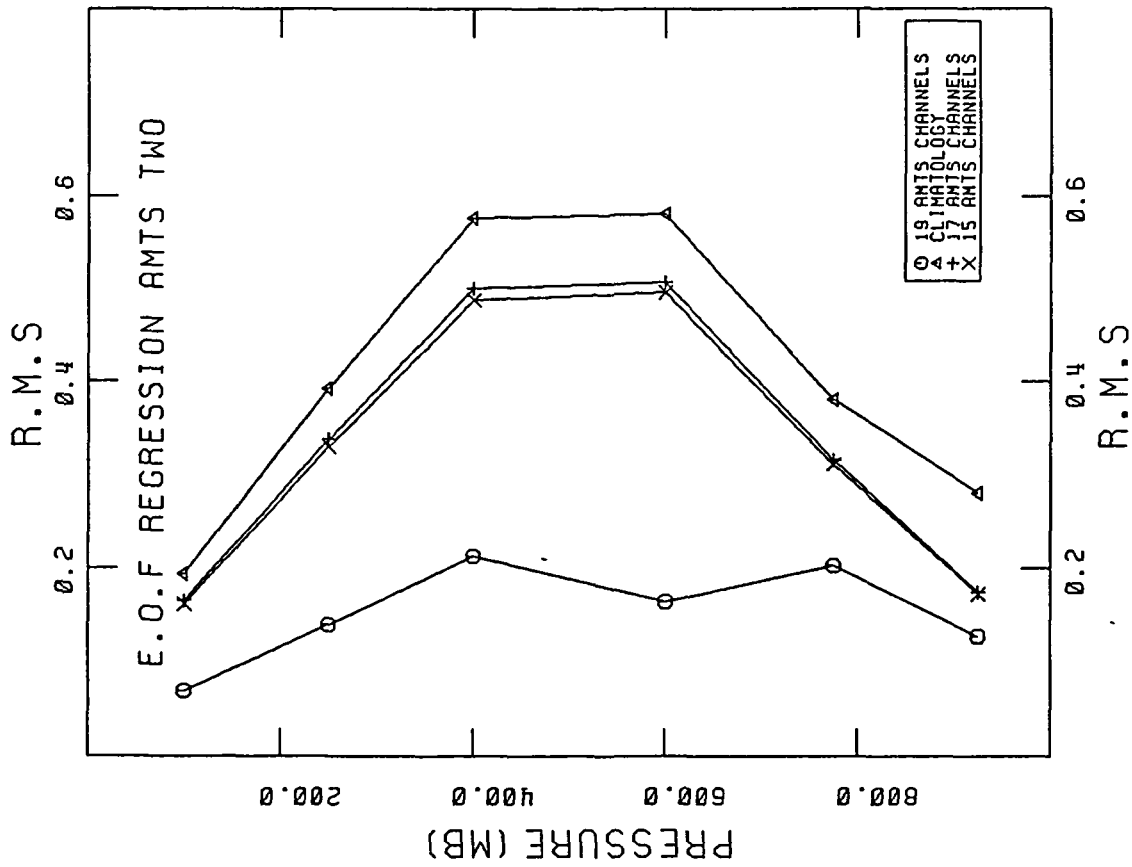
Figure 5-6. RMS errors for TWO and MWM statistical retrievals with all 19 AMTS temperature channels, with channels 1 and 2 missing, with channels 1, 2, 3, and 28 missing, and for climatology.

6. SUMMARY AND CONCLUSIONS

A two-step method has been developed to retrieve water vapor profiles from satellite radiance data employing a physically-based first guess initialization of an inversion of the radiative transfer equation by relaxation. The approach has been applied to synthetic radiance data calculated for water vapor channels of the HIRS and AMTS instruments for ensembles of seasonally and latitudinally dependent radiosondes. Results of these simulated retrievals are summarized in Table 6 for the two sounding sets corresponding to the most and least successful performance, i.e. tropical ocean winter (TWO) and midlatitude winter (MW), respectively. For each layer and instrument the fraction of unexplained variance (FUV) has been evaluated corresponding to both first guess retrievals alone and those obtained after subsequent relaxation. The FUV values correspond to the ratio of variance remaining after retrieval to that of the original climatology. Meaningful values lie between 0 and 1, corresponding to perfect and perfectly useless, retrievals, respectively. To compare the two instruments, the ratio of FUVs for HIRS and AMTS is included to provide a figure of merit (FOM) indicating the relative ability of the AMTS to decrease the unexplained variance. The FOM is unity when the instruments perform equally and greater than unity when AMTS outperforms HIRS.

From these values it is notable that even the first guess procedure alone provides skillful retrievals for layers in the middle atmosphere. The greatest reduction in variance occurs for the AMTS-based retrievals in the 300-500 mb layer. Using relaxed retrievals, the FUV is reduced even further. From the FOM values, it appears that the high resolution AMTS water vapor channels are capable of reducing the unexplained variance by factors of at least 1.5 and usually greater than 2.0 relative to the HIRS-2 system.

The results of statistical inversion simulations show that better retrievals should be obtainable in the lowest and highest layers, where the simulated physical retrievals were the poorest, and where better retrieval algorithms and/or better channels seem to be required. The use of moisture-sensitive channels in the 15 μm CO_2 band to retrieve low layer water vapor seems particularly promising.

Table 6. First Guess and Relaxation FUV and FOM Values

Sounding Set: Layer	First Guess			Relaxed		
	FUV (HIRS)	FUV (AMTS)	FOM	FUV (HIRS)	FUV (AMTS)	FOM
(a) TWO						
< 200	1.50	1.24	1.2	0.90	0.27	3.3
200-300	0.81	0.15	5.4	0.03	0.02	1.5
300-500	0.21	0.08	2.6	0.17	0.02	8.5
500-700	0.37	0.14	2.6	0.32	0.06	5.3
700-1000	0.63	0.90	0.7	0.55	0.31	1.8
(b) MW						
< 200	25.12	8.50	2.9	5.52	1.19	4.6
200-300	0.72	0.25	2.9	0.08	0.04	2.0
300-500	0.28	0.07	4.0	0.16	0.05	3.2
500-700	1.26	0.35	3.6	1.33	0.30	4.4
700-1000	1.53	0.13	11.8	1.77	0.77	2.3

The usefulness of the 700 and 650 cm^{-1} channels to obtain water retrievals in the upper troposphere and lower mid-latitude and polar stratosphere cannot be adequately tested against radiosonde measurements because radiosondes do not measure water vapor above about the 300 mb level. Hopefully, the new ATMOS data will provide measurements at these heights against which to test retrievals from the new channels, which promise to extend the height to which the atmosphere is routinely sounded for water vapor.

ACKNOWLEDGEMENTS

MEETINGS ATTENDED

Dr. Kaplan attended the NASA/IFAORS Review of Instrument Development in the Global Scale Process Research Program held in Washington, D.C. on September 26 and 27, 1983, and presented a report on "AMTS Studies", with emphasis on the H_2O channels including the weighting functions and sensitivity analysis of the new set of channels. He also attended the Fifth AMS Conference on Atmospheric Radiation held in Baltimore, MD, October 31 to November 4, 1983, and co-chaired a session on Radiation and GCM. A paper entitled "Retrieval of Humidity Profiles from Satellite Radiance Measurements" by L. D. Kaplan and R. G. Isaacs was presented at the Workshop on Advances in Remote Sensing Retrieval Methods, held in Williamsburg, VA, October 30 to November 2, 1984. It will appear in Advances in Remote Sensing Retrieval Methods, published by A. Deepak Publishing and edited by A. Deepak, H. E. Fleming, and M. T. Chahine. Reprints will be sent when they are available.

REFERENCES

Chahine, M. T., 1968: Determination of the temperature profile in an atmosphere from its outgoing radiance. J. Opt. Soc. Amer., 58, 1634-1637.

Chahine, M. T., 1970: Inverse problems in radiative transfer: Determination of atmospheric parameters. J. Atmos. Sci., 27, 960-967.

Chahine, M. T., N. L. Evans, V. Gilbert, and R. D. Haskins, 1984: Requirements for a passive IR advanced moisture and temperature sounder. Appl. Opt., 23, 7, 979-989.

Clough, S. A., 1983: Preliminary Instructions for FASCOD1C (rev. 1). AFGL/OPI, 27 September 1983, 26 pp.

Gaut, N. E., and E. C. Reifenstein III, 1971: Interaction model of microwave energy and atmospheric variables. ERT Tech. Rep. No. 13, Environmental Research and Technology, Inc., Waltham, MA, 167 pp.

Isaacs, R. G., G. Deblonde, R. D. Worsham, M. Livshits, 1985: Millimeter wave moisture sounder feasibility study: The effect of cloud and precipitation on moisture retrievals. AFGL TR-85-0040, Air Force Geophysics Laboratory, Hanscom AFB, Bedford, MA 01731.

Gaut, N. E., 1967: Studies of Atmospheric Water Vapor by Means of Passive Microwave Techniques, Ph.D. Thesis, Dept. of Meteor. M.I.T., Cambridge, MA.

Gaut, N. E., 1968: Research Laboratory of Electronics Tech. Report No. 467, M.I.T., Cambridge, MA.

NOAA, 1981: NOAA Polar Orbiter Data (TIROS-N and NOAA-6) Users' Guide. NOAA-EDIS-NCC-SDSD, Washington, DC.

Phillips, N. A., 1984: Results of Comparative Simulation Studies on AMTS and HIRS Conducted by NASA and NOAA (to be published).

Rigone, J. L. and A. P. Stogryn, 1977: Data processing for the DMSP microwave radiometer system. In Proc. Eleventh International Symp. Remote Sensing of the Environment. Univ. of Michigan, Ann Arbor, MI, pp. 1599-1608.

Rodgers, C. D., 1966: A Discussion of Inversion Methods, Memo 66.13, Clarendon Laboratory, Oxford University.

Rodgers, C. D., 1967: The radiative heat budget of the troposphere and lower stratosphere. MIT Department of Meteorology, Report No. A2, Cambridge, MA.

Rosenberg, A., D. B. Hogan, C. K. Bowman, 1983: Satellite Moisture Retrieval Techniques. Vol. 1: Technique Development and Evaluation. CR 83-01(a), Naval Environmental Prediction and Research Facility, Monterey, CA 93940.

Rosenberg, P. W., M. J. Konichak, and D. H. Staelin, 1982: A method for estimation of atmospheric water vapor profiles by microwave radiometry. J. Appl. Meteor., 21, 1364-1370.

Rosenkranz, P. W., M. J. Komichak, and D. H. Staelin, 1982: A method for estimation of atmospheric water vapor profiles by microwave radiometry. J. Appl. Meteorol., 21, 1364-1370.

Rothman, L. S., R. R. Gamache, A. Barbe, A. Goldman, J. R. Gillis, L. R. Brown, R. A. Toth, J.-M. Flaud, and C. Camy-Peyret, 1983: AFGL atmospheric line parameters compilation. Appl. Opt., 22, 2247-2256.

Smith, H. J. P., D. J. Dube, M. E. Gardner, S. A. Clough, F. X. Kneizys, and L. S. Rothman, 1978: FASCODE - Fast atmospheric signature code (spectral transmittance and radiance).

Smith, W. L., H. M. Woolf, C. M. Hayden, D. Q. Wark, and L. M. McMillan, 1979: The TIROS-N operational vertical sounder. Bull. Am. Meteorol. Soc., 60, 1177-1187.

Smith, W. L., and H. M. Woolf, 1976: The use of eigenvectors of statistical covariance matrices for interpreting satellite sounding radiometer observations. J. Atmos. Sci., 33, 1127-1140.

Staelin, D. H., 1967: Quarterly Progress Report No. 85, Research Laboratory of Electronics, M.I.T., Cambridge, MA, April 15, pp. 15-16.

Susskind, J., and J. E. Searl, 1978: Synthetic atmospheric transmittance spectra near 15 μm and 4.3 μm. J. Quant. Spectrosc. Radiat. Trans., 19, 195-215.

Susskind, J., J. Rosenfield, D. Reuter, and M. T. Chahine, 1982: The GLAS physical inversion method for analysis of HIRS-2/MSU sounding data. NASA-TM-84936, 101 pp.

Waters, J. W. and D. H. Staelin, 1968: Quarterly Progress Report No. 89. Research Laboratory of Electronics, M.I.T., Cambridge, MA, April 15, pp. 25-28.

Westwater, E. R. and O. N. Strand, 1965: Application of Statistical Estimation Techniques to Ground-Based Passive Probing of the Tropospheric Structure, ESSA Technical Report No. IER 371/1TSA 37.